Project number: 101111888
Project acronym: SHIMMER
Project duration: 09/2023 – 08/2026
Project Coordinator:
Andrea Alvarado Shmueli, SINTEF AS – Institute SINTEF Industry

Co-funded by the European Union

HORIZON 2020: Horizon Europe Framework Programme (HORIZON)

HORIZON-JTI-CLEANH2-2022-05-03

Safe hydrogen injection management at network-wide level: towards European gas sector transition

Shimmer

Safe Hydrogen Injection Modelling and Management for European gas network Resilience

D4.6 Report on parametric analysis and out-of-domain generalization of results.

Analysis and guidelines for smart network operation

VERSION	DATE	TYPE	DISSEMINATION LEVEL
Version 1.3	09-03-2026	Report	Public

ABSTRACT

This deliverable presents a methodological framework for the parametric analysis and out-of-domain generalization of gas network simulations under hydrogen blending conditions. The proposed approach combines high-fidelity steady state physical gas network modelling with a vector-valued Kernel Ridge Regression (KRR) surrogate model, enabling fast prediction of fluid-dynamic variables and subsequent hydrogen concentration tracking through a dedicated mixing module.

The methodology has been tested on both TSO and DSO network (Snam and InRete real networks). It has been demonstrated on a real DSO network (Riccione, Italy) and progressively tested under increasing parametric dimensionality, from 4 up to 30 independent input parameters, including inlet pressure set-points, hydrogen blending fractions, pipeline roughness, and distributed gas consumptions.

Results show that the surrogate-based workflow drastically reduces computational time while preserving predictive accuracy, enabling large-scale Monte Carlo simulations and Global Sensitivity Analysis. The global sensitivity analysis allows the assessment of the most impactful input parameters on the nodal hydrogen concentration of each node.

The framework allows the identification of homogeneous gas quality areas, mixing zones, and moving concentration boundaries, providing quantitative support for smart hydrogen blending management and network-wide gas quality control.

AUTHORSHIP AND APPROVAL INFORMATION

AUTHOR(S)
Marco Cavana / PoliTo
Riccardo Trinchero / PoliTo
Paolo Manfredi / PoliTo
Davide Rubinetto / PoliTo
Igor Stievano / PoliTo
Pierluigi Leone / PoliTo

DATE / SIGN
09/03/2026

REVIEWED BY WP-LEADER
Huib Blokland / TNO

DATE / SIGN
09/03/2026
Huib Blokland
Huib Blokland (Mar 9, 2026 14:45:41 GMT+1)

APPROVED BY COORDINATOR
Diana González / SINTEF

DATE / SIGN
09/03/2026
Diana González
Diana Gonzalez (Mar 9, 2026 14:48:59 GMT+1)

FUNDED BY THE EUROPEAN UNION. VIEWS AND OPINIONS EXPRESSED ARE HOWEVER THOSE OF THE AUTHOR(S) ONLY AND DO NOT NECESSARILY REFLECT THOSE OF THE EUROPEAN UNION OR THE CLEAN HYDROGEN JOINT UNDERTAKING. NEITHER THE EUROPEAN UNION NOR THE GRANTING AUTHORITY CAN BE HELD RESPONSIBLE FOR THEM.

Release history

VERSION	DATE	VERSION DESCRIPTION
0.1	09-12-2025	First draft – work in progress
1.0	13-02-2026	Version sent to internal review
1.1	16-02-2026	Version sent for review to project partners
1.2	03-03-2026	Revised version
1.3	09-03-2026	Final version for submission after last minor revision and data confidentiality check

The research leading to these results has received funding from Horizon 2020, the European Union's Framework Programme for Research and Innovation (H2020) under grant agreement n° 101111888.

Table of contents

The research leading to these results has received funding from Horizon 2020, the European Union's Framework Programme for Research and Innovation (H2020) under grant agreement n° 101111888.

The research leading to these results has received funding from Horizon 2020, the European Union's Framework Programme for Research and Innovation (H2020) under grant agreement n° 101111888.

Table of Figures

The research leading to these results has received funding from Horizon 2020, the European Union's Framework Programme for Research and Innovation (H2020) under grant agreement n° 101111888.

The research leading to these results has received funding from Horizon 2020, the European Union's Framework Programme for Research and Innovation (H2020) under grant agreement n° 101111888.

List of Tables

The research leading to these results has received funding from Horizon 2020, the European Union's Framework Programme for Research and Innovation (H2020) under grant agreement n° 101111888.

List of Abbreviations

Table 1: List of abbreviations

Term	Explanation
DSO	Distribution System Operator
TSO	Transmission System Operator
ML	Machine Learning
KRR	Kernel Ridge Regression
MC	Monte Carlo
RMSE	Root Mean Square Error
PDF	Probability Density Function
FRS	Final Reduction Stations

The research leading to these results has received funding from Horizon 2020, the European Union's Framework Programme for Research and Innovation (H2020) under grant agreement n° 101111888.

Executive Summary

Traditional case-specific studies in gas network analysis provide valuable insights but often lack a systematic and quantitative assessment when key parameters defining network behaviour – such as inlet pressure set-points, user consumptions, technical parameters and, in future, hydrogen blending levels – vary simultaneously. This deliverable addresses this limitation by developing and validating a scalable surrogate-based framework for parametric and statistical analysis of gas networks under hydrogen blending conditions.

The proposed methodology combines steady state gas network simulations from physical models with vector-valued Kernel Ridge Regression (KRR) surrogate modelling and statistical analysis. The surrogate accurately reproduces fluid-dynamic variables (pressures, flow rates, velocities, and nodal gas exchanges), which are then used within a dedicated mixing module to compute hydrogen concentrations. Validation results across all investigated scenarios—including the most complex 30-parameter independent variables case with independent inlet pressures set points and independent variation of distributed consumption clusters – show strong agreement with the physical model. Hydrogen concentration prediction errors remain below approximately 1% RMSE even for the worst nodes, confirming robustness even in high-dimensional settings.

A key advance demonstrated in this work is the drastic reduction in computational burden. Large Monte Carlo campaigns that would require several hours with the physical solver can be replaced by surrogate evaluations completed in milliseconds. This enables systematic parametric exploration, uncertainty quantification, and variance-based Global Sensitivity Analysis, which would otherwise be impractical in an operational context.

The framework allows the evaluation of multiple hydrogen blending injection points with independently varying concentration levels, pressure set points and geographically distributed consumption variations. Results consistently show that the network organizes into quasi-homogeneous gas quality areas separated by transitional zones corresponding to moving concentration boundaries. Sensitivity analyses confirm that hydrogen concentration at injection points is the primary driver of nodal composition, while inlet pressure set-points represent the dominant fluid-dynamic control variable governing spatial propagation and mixing behaviour. Consumption clusters exert a localized, topology-dependent influence.

When extending the analysis to out-of-domain scenarios with uncorrelated parameter variations, the critical areas identified in simpler cases persist, although with increased spatial diffusion. This demonstrates the generalization capability of the approach.

Overall, this deliverable transforms hydrogen blending assessment from deterministic scenario testing into a probabilistic, sensitivity-driven evaluation framework, providing quantitative support for identifying homogeneous quality areas, localizing critical mixing and/or transition zones, and enabling informed operational decision-making in multi-gas networks.

About the project: The European natural gas infrastructure provides the opportunity to accept hydrogen (H_2), as a measure to integrate low-carbon gases while leveraging the existing gas network and contributing to decarbonisation. However, there are technical and regulatory gaps that should be closed, adaptations and investments to be made to ensure that multi-gas networks across Europe will be able to operate in a reliable and safe way while providing a highly controllable gas quality and required energy demand. Aspects such as material integrity of pipelines and components, as well as the lack of harmonisation of gas quality requirements at European level must be addressed in order to facilitate the injection of H_2 in the natural gas network.

In this context, the SHIMMER project (Safe Hydrogen Injection Modelling and Management for European gas network Resilience) was selected for funding as part of the 2023 Clean Hydrogen Partnership programme. SHIMMER aims to enable a higher integration of low-carbon gases and safer H_2 injection management in multi-gas networks by strengthening the knowledge base and improving the understanding of risks and opportunities in H_2 projects.

The research leading to these results has received funding from Horizon 2020, the European Union's Framework Programme for Research and Innovation (H2020) under grant agreement n° 101111888.

It will do this by:

- Mapping and assessing European gas T&D infrastructure in relation to materials, components, technology, and their readiness for hydrogen blends.
- Defining methods, tools and technologies for multi-gas network management and quality tracking, including simulation, prediction, and safe management of network operation in view of widespread hydrogen injection in a European-wide context.
- Proposing best practice guidelines for handling the safety of hydrogen in the natural gas infrastructure and managing the risks.

The research leading to these results has received funding from Horizon 2020, the European Union's Framework Programme for Research and Innovation (H2020) under grant agreement n° 101111888.

1 Introduction

1.1 Purpose of the document

This deliverable documents the development and application of a statistical and surrogate-based framework for the parametric analysis and generalization of gas network simulations under hydrogen blending conditions. It reports the activities carried out within Task 4.3.2, focusing on the systematic exploration of how variations in operational set-points, design parameters, and hydrogen injection levels affect fluid-dynamic variables and gas quality distribution across a gas network.

The main purpose of this document is to:

- Present the methodological workflow combining high-fidelity gas network simulations, vector-valued Kernel Ridge Regression (KRR) surrogate modelling, Monte Carlo analysis, and Global Sensitivity Analysis;
- Demonstrate the applicability of the proposed approach on a real gas network (Riccione case study);
- Assess the robustness of the methodology when increasing the dimensionality of the parametric space, including out-of-domain operating scenarios;
- Provide quantitative insights and operational guidelines for smart hydrogen injection management and gas quality tracking under increasing complexity case studies.

Within the overall SHIMMER project structure, this deliverable contributes to the development of advanced modelling and decision-support tools for multi-gas network management. It builds upon previous deliverables addressing network modelling and hydrogen blending simulation (e.g. D4.1, D4.4) and provides methodological foundations that can support subsequent work related to network operation strategies, and best-practice guidelines.

1.2 Intended readership

This deliverable is primarily addressed to:

- Distribution System Operators (DSOs) and Transmission System Operators (TSOs) interested in understanding how hydrogen blending variability propagates through real networks depending on fluid-dynamic operating set-points and technical features, and how uncertainties on these parameters influence gas quality distribution;
- Technical experts and engineers involved in gas network modelling, hydrogen integration studies, and operational planning;
- Researchers and technology developers working on surrogate modelling, uncertainty quantification, and data-driven approaches applied to energy infrastructures;
- Policy makers and regulatory stakeholders, who require quantitative evidence on the controllability and predictability of hydrogen blending in existing gas infrastructures.

For network operators, the document provides a structured methodology to move from deterministic scenario analysis toward probabilistic and sensitivity-based evaluation of hydrogen injection strategies. For researchers, it offers a reproducible workflow integrating machine learning with physics-based simulation for high-dimensional, vector-valued engineering problems. For regulators and policy actors, it contributes to a better understanding of how hydrogen concentration areas within the same infrastructure may evolve under varying operating conditions and how such behaviour can be quantified, managed and accepted (e.g. by institution of hydrogen concentration variation acceptability ranges).

The research leading to these results has received funding from Horizon 2020, the European Union's Framework Programme for Research and Innovation (H2020) under grant agreement n° 101111888.

1.3 Structure of this document

This document is structured to guide the reader from the problem definition to the application and generalization of results.

- **Chapter 2** introduces the background and motivation, clarifying the challenges associated with hydrogen blending and the need for parametric and statistical approaches.
- **Chapter 3** describes the case study network and the investigated scenarios, including no-blending and hydrogen blending cases with increasing parametric dimensionality.
- **Chapter 4** presents the methodological framework, including the modelling workflow, surrogate model formulation, and global sensitivity analysis.
- **Chapter 5** reports and discusses the results obtained for the different test cases, with particular emphasis on hydrogen concentration distribution, mixing behavior, moving boundaries, and out-of-domain generalization.
- **Chapter 6** draws the main conclusions and outlines directions for further work.
- The **Appendix** provides the mathematical formulation of the compressed vector-valued KRR approach and a pseudocode representation of the machine-learning workflow.

This structure allows readers to separately access the methodological developments and the application-oriented results, depending on their specific interest.

1.4 Stakeholder involvement

The methodology has been tested on both TSO and DSO real networks (Snam and InRete networks) and then it has been demonstrated on the network of InRete (DSO).

During the testing phase, a portion of the Sicily network from Snam has been used following the same procedures and rationale as for the InRete one, bringing to the same results. These have been presented in the project milestone M9. Testing on the Snam network has been omitted here for the sake of conciseness, as does not add relevant additional information.

The case study network is based on real infrastructure data provided by a Distribution System Operator (INRETE Distribuzione Energia S.p.A.), ensuring that the modelling assumptions and parameter ranges reflect realistic operational conditions. The definition of operational scenarios, including hydrogen injection ranges and pressure set-point variations, has been aligned with practical considerations from network operation and hydrogen integration perspectives.

Within the SHIMMER consortium, the methodology and intermediate results have been presented and discussed with research partners within WP4.

Although the methodological development is primarily research-oriented, the framework has been designed with practical applicability in mind, particularly with respect to gas quality monitoring strategies, definition of homogeneous composition areas, and identification of critical transitional nodes. This ensures alignment with the broader SHIMMER objective of enabling safe and controllable hydrogen injection management in European gas networks.

The research leading to these results has received funding from Horizon 2020, the European Union's Framework Programme for Research and Innovation (H2020) under grant agreement n° 101111888.

2 Background and motivation

Gas transmission and distribution networks are complex, interconnected systems comprising hundreds of nodes, pipelines, and auxiliary components such as compressors, regulators, valves and interconnections with other network subsystems. The possibility of injecting hydrogen and blending it within natural gas is seen as a way to start the hydrogen economy, to use already existent assets and contributing to the decarbonization of the overall energy system. However, this poses a number of challenges on the acceptability of shares of hydrogen by the overall natural gas system, from infrastructure material compatibility to suitability with final appliances and metering and billing issues. From a Transmission and Distribution System Operator perspective, this translates into a challenge of management of the gas quality throughout their networks. This, in turn, calls for the need of gas networks simulations capable to calculate the gas quality tracking the hydrogen presence and spreading. The need to control gas quality by network operators is stated also in the technical norm EN 16726:2025 – "Gas Infrastructure – Quality of gas – Group H" which specify the gas quality characteristics, their acceptable range and inform on the challenges to set acceptable rate of change in Wobbe Index value. The topic is addressed in Annex F (informative), highlighting how the spreading of distributed sources of gas from different origin may bring out the issue of gas quality management of networks, even at distribution level.

Under distributed hydrogen (H_2) injection, accurate simulations rely on physics-based models capable of accounting for variations in design parameters (e.g., pipe sizing, pipeline roughness), variations in operational set points (e.g. pressure set points) and uncertain boundary conditions (e.g., demand profiles). Although detailed numerical simulations provide high-fidelity results, they are computationally demanding. Running multiple simulations to explore different configurations or scenarios significantly increases computational time and often requires extensive manual intervention. These kinds of generalized and network wide scenario analysis, when dealing with hydrogen blending are key to understand how the infrastructure behaves and, overall, how the hydrogen-natural gas mixture spreads over the network over a range of possible operational and design conditions.

This report is part of Task 4.3.2 of the SHIMMER project, and addresses these challenges by developing a framework to systematically evaluate how variations in network design and operation, affect overall performance especially those related to H_2 blending spreading over the network. Key aspects include the number and concentration of hydrogen injection points, as well as uncertainties in gas consumption at individual nodes or consumption clusters, and their effects on pressures, flow rates, velocities, and nodal concentration map.

The research objectives of this task are:

- Generalization of results from gas network fluid-dynamic simulation of operational strategies with physical parameters variation;
- Choice of suitable tools for parametric analysis;
- Testing of proposed solution on a subset of real case networks;
- Results elaboration to find generalization pattern.

The task focuses particularly on providing a methodological approach and a sample test to answer the following question:

- How hydrogen admixing within a network infrastructure is affected by the main regulated (e.g. pressure set points) and un-regulated (final consumption) parameters and design parameters?

The research leading to these results has received funding from Horizon 2020, the European Union's Framework Programme for Research and Innovation (H2020) under grant agreement n° 101111888.

To mitigate the computational cost of exhaustive simulation campaigns, the task integrates ML techniques to automate and accelerate the parametric analysis of network behaviour. A surrogate model is developed from a representative set of high-fidelity simulations, capturing variations in the most relevant design and operational parameters. Based on a multi-output formulation of the Kernel Ridge Regression (KRR), the surrogate provides a fast analytical approximation of the network's response. Once trained, it predicts key outputs– such as node pressures – in a fraction of a second, enabling large-scale statistical evaluations of the network performance.

Although the application of machine-learning techniques to energy networks has received increasing attention in recent years, comparatively little effort has been devoted to quality tracking [1-5]. The proposed methodology is shown to effectively address this gap.

2.1 Problem Statement

As illustrated in Figure 2-1, a gas network typically consists of hundreds of nodes, pipes, and auxiliary components. The key output variables of interest, such as node pressure, pipe flow rate, velocity, and hydrogen concentration – are collected in the output vector $\boldsymbol{y}$, forming a vector-valued problem that is inherently challenging due to the multidimensional nature of the outputs. The objective is to develop a predictive model $\widetilde{\boldsymbol{\mathcal{M}}}$, hereafter referred as surrogate model, able to estimate the output vector $\boldsymbol{y}$ as a function of any configuration of the input parameters $\boldsymbol{x}$ in a given domain, including inlet pressure, gas consumption, hydrogen concentration, pipe roughness, and diameters that constitute a heterogeneous set of influencing variables. The above regression problem turns out to be vector-valued problem that is inherently challenging due to the multidimensional nature of the outputs.

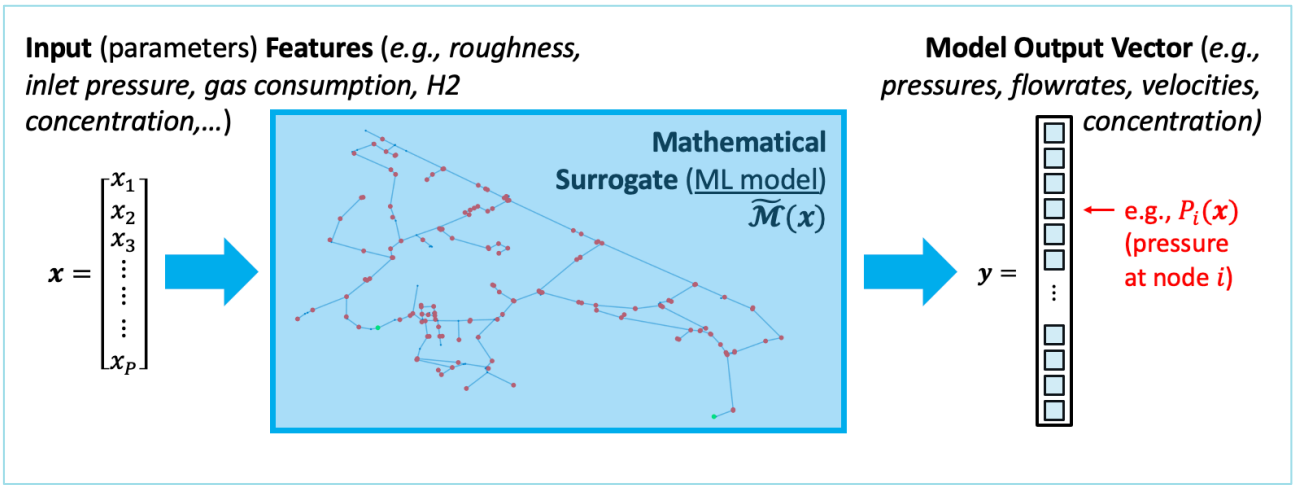

Figure 2-1: definition of the main output variables in a gas network, including node pressures, pipe flow rates, velocities, and hydrogen (H2) concentrations, all stored in vector $\boldsymbol{y}$. The figure also illustrates the concept of generating a ML-based mathematical model to approximate the network behaviour through a compact and efficient relation $\boldsymbol{y} \approx \widetilde{\boldsymbol{\mathcal{M}}}(\boldsymbol{x})$, where $\boldsymbol{x}$ represents the configuration of the selected input parameters.

The goal is to build a surrogate model $\widetilde{\boldsymbol{\mathcal{M}}}(\boldsymbol{x})$, capable of accurately reproducing network behaviour, from a limited number of training data (i.e., numerical simulations) using a ML regression.

The research leading to these results has received funding from Horizon 2020, the European Union's Framework Programme for Research and Innovation (H2020) under grant agreement n° 101111888.

The selection of suitable ML and statistical techniques is guided by both the problem characteristics and the expertise of the Polito research team [6,7,8]. Among the available approaches, artificial neural network and deep learning architectures are particularly flexible and effective at capturing complex nonlinear relationships, as widely demonstrated in pattern recognition tasks. However, their training typically requires large datasets (often comprising thousands of samples) and substantial computational resources, including graphical processing units and parallel computing capabilities. Unlike fields such as computer vision, where large datasets are readily available, generating sufficient data for engineering applications is often computationally demanding and costly.

Kernel-based methods offer an attractive alternative for surrogate modelling. While less flexible than neural networks and not inherently designed for vector-valued regression problems in their plain implementations available in commercial and open-source toolboxes, they present significant advantages: 1) a linear model structure with convex optimization, 2) straightforward training without specialized hardware, and 3) strong performance with small training sets. Multi-output extensions of kernel regression have been successfully demonstrated in recent studies [6], confirming their suitability for complex vector-valued problems such as the modelling of gas networks. Thanks to their ability to learn effectively from limited data while maintaining high computational efficiency, kernel methods provide a robust and promising solution for developing surrogate models that accurately reproduce network behaviour under varying conditions, enabling comprehensive statistical analysis and deeper insight into system variability.

The research leading to these results has received funding from Horizon 2020, the European Union's Framework Programme for Research and Innovation (H2020) under grant agreement n° 101111888.

3 Case study and scenarios

The methodology developed in this deliverable is fully applicable to both Transmission (TSO) and Distribution (DSO) gas networks. The approach has been tested on a representative TSO case within a project milestone (MS9), confirming that no methodological differences arise between transmission and distribution applications. Testing on the Snam network has been omitted here for the sake of conciseness, as does not add relevant additional information. In this way, the report addresses consistently one representative case of distribution networks, showcasing methodology for the control of gas quality at distribution level, which is not common at present but a challenge if hydrogen and other renewable gases will be injected at local level.

The surrogate-based modelling framework, mixing formulation, and sensitivity analysis are topology-independent and rely on general network equations common to both systems. Therefore, once validated, the methodology can be directly transferred to TSO networks without structural modifications, more precisely to the portion of transmission system where non-pipeline elements such as compressors and pressure regulation stations are not present..

For the purpose of producing a comprehensive report with extensive scenario variations—ranging from 4 to 30 independent parameters and including multiple hydrogen injection configurations—the effort was concentrated on a well-characterized DSO case. This allowed a deeper and more systematic exploration of parametric effects, mixing patterns, and moving concentration boundaries, while preserving full methodological generality. What is more, according to the technical norm EN 16726 (2025) about gas quality in the gas infrastructure, one of the mitigation strategies for the abrupt variations in gas quality within the network (which can cause problems to final appliances) is the flow controls and quality management in the grid at DSO level, implying that it is a portion of the infrastructure which requires more focus than the TSO's one.

3.1 Network description

This task focuses primarily on the parametric analysis over gas distribution networks. Among the real DSO networks available, the one provided by INRETE Distribuzione Energia S.p.A. has been addressed as a sample case. The distribution infrastructure is the one of the city of Riccione, Italy, and has already been described in Deliverable D4.1.

It is composed of two pressure tiers: 5 – 1.5 bar_g (4^{th} species [1]) and <0.04 bar_g (7^{th} species), following the Italian classification of pressure level. Overall, it serves about 23,000 final users and it is fed by two city-gates (Regulation and Metering station – ReMi in the Italian jargon) which are connected to the transmission system.

In this task, we focused on the higher-pressure tier only. The topology of the addressed infrastructure is given in Figure 3-1.

The red squares in the map represents the 24 final gas pressure reduction stations (FRS), which are the interconnecting plants between the higher and the lower pressure grid. These are the main gas exit points from the piece of infrastructure considered and, later in the sample case studies, they will be considered as "aggregated consumption points". From a topological point of view, the network database consists of 249 pipelines and 241 nodes. Out of these 241 nodes, 110 are additional consumption points directly connected to the 4^{th} species pipeline system. The nominal values of the main operational settings are as follows: entry pressure at the Primary ReMi station: 4.5 bar; entry pressure at the Secondary ReMi station: 4.1 bar; exit flow FRS to Riccione users: as provided by the DSO.

[1] In the Italian gas network, the pipelines are classified into seven "species" according to their maximum operating pressure: from above 24 bar_g (1^{st} species) to less than 40 $mbar_g$ (7^{th} species). Typically, the DSOs operate networks composed of pipelines classified from the 4^{th} species downwards.

The research leading to these results has received funding from Horizon 2020, the European Union's Framework Programme for Research and Innovation (H2020) under grant agreement n° 101111888.

Figure 3-1: higher-pressure level of the natural gas distribution infrastructure of Riccione (INRETE) considered in this deliverable.

The Riccione case study is particularly relevant because it allows us to explore the consequences of hydrogen blending for an interconnected distribution network with two inlet points and a mild looped topology.

The final aim is to generate a surrogate model of the gas network able to cover a wide range of operational conditions, allowing parametric and statistical analysis of the following network-wide outputs:

- Nodal pressure parametric variation and sensitivity;
- Pipeline velocity parametric variation and sensitivity;
- Localization of mixing points and its parametric variation;

In relation to the variation of each input parameter, with particular focus on the effects of hydrogen presence throughout the network, a sensitivity analysis of the output variables (i.e., pressures, velocities, and hydrogen fractions) with respect to the inputs is performed. The relative contribution of each input parameter to the variability of each output is evaluated and quantified. This allows the identification of the input parameters whose variations most significantly influence the selected output response. This is achieved via the so-called Global Sensitivity Analysis, illustrated in the last part of the next chapter.

The research leading to these results has received funding from Horizon 2020, the European Union's Framework Programme for Research and Innovation (H2020) under grant agreement n° 101111888.

3.2 Scenarios list and description

The proposed modeling scheme and statistical analysis will be tested on the following scenarios

1) No-H_2 blending cases: in order to showcase the workflow and the key method features.
   Within this scenario, two sub-cases are addressed:
   a) 4 input parameter test case:
      - Par.1) Entry pressures at both ReMi stations (with a variation $\Delta P = \pm 7$ %);
      - Par.2) Pipeline diameters ($\Delta D = \pm 5$ %);
      - Par.3) Pipeline roughness ($\Delta E = \pm 10$ %);
      - Par.4) Exit flow to Riccione users ($\Delta G_{ext} = \pm 20$ %). In the first application, this parameter affects all exit flows equally, causing them to vary by the same amount.
   b) 29 input parameter test case:
      - Par.1) Entry pressures at ReMi station 1 (with a variation $\Delta P = \pm 7$ %);
      - Par 2) Entry pressures at ReMi station 2 (with a variation $\Delta P = \pm 7$ %);
      - Par.3) Pipeline diameters ($\Delta D = \pm 5$ %);
      - Par.4) Pipeline roughness ($\Delta E = \pm 10$ %);
      - Par.5-29) Exit flow to Riccione clusters of users ($\Delta G_{ext} = \pm 20$ %): each cluster is represented by one final reduction station (FRS) plus a cluster of composed by all the users directly connected to the higher-pressure tier. Being each of this cluster associated with a parameter, it allows the independent variation of each exit point, increasing the model complexity and the applicability range.

In these preliminary cases, the pipeline diameters have been considered as an input variable to stress and test the methodology including variations on a design variable (rather than only operational variables). In the following cases, the pipeline diameters have not been considered anymore to simplify the domain of variation to a more realistic set of cases where the changing variables are the typical operation set points together with the blending shares.

2) H_2 blending cases:
   a) 4 input parameters with one hydrogen injection:
      - Par.1) Entry pressures at both ReMi stations (with a variation $\Delta P = \pm 7$ %);
      - Par.2) H2 blending at the primary ReMi station ($10\%_{mol} \pm \Delta H = \pm 95$ %)[2];
      - Par.3) Pipeline roughness ($\Delta E = \pm 10$ %);
      - Par.4) Exit flow to Riccione users ($\Delta G_{ext} = \pm 20$ %).
   b) 5 input parameters with two hydrogen injection:
      - Par.1) Entry pressures at both ReMi stations (with a variation $\Delta P = \pm 7$ %);
      - Par.2) H2 blending at the primary ReMi station ($10\%_{mol} \pm \Delta H = \pm 95$ %);
      - Par.3) H2 blending at the primary ReMi station ($10\%_{mol} \pm \Delta H = \pm 95$ %)
      - Par.4) Pipeline roughness ($\Delta E = \pm 10$ %);
      - Par.5) Exit flow to Riccione users ($\Delta G_{ext} = \pm 20$ %).
   c) 30 input parameters test case with two hydrogen injection:
      - Par.1) Entry pressures at ReMi station 1 (with a variation $\Delta P = \pm 7$ %);
      - Par 2) Entry pressures at ReMi station 2 (with a variation $\Delta P = \pm 7$ %);
      - Par.3) H2 blending at the primary ReMi station ($10\%_{mol} \pm \Delta H = \pm 95$ %);
      - Par.4) H2 blending at the primary ReMi station ($10\%_{mol} \pm \Delta H = \pm 95$ %)
      - Par.5) Pipeline roughness ($\Delta E = \pm 10$ %);
      - Par.6-30) Exit flow to Riccione clusters of users ($\Delta G_{ext} = \pm 20$ %).

[2] The hydrogen concentration variation is in the following range: [0.5% ÷ 19.5%]

The research leading to these results has received funding from Horizon 2020, the European Union's Framework Programme for Research and Innovation (H2020) under grant agreement n° 101111888.

For both the set of cases, the nominal values are summarized hereafter:

- Pressure of the primary ReMi Station $P_1 = 4.5\ bar_g$
- Pressure of the secondary ReMi Station $P_2 = 4.1\ bar_g$
- Pipeline roughness $\varepsilon = 140\ \mu m$ – value from the DSO, typical for old steel pipelines.
- Pipeline diameters D in the range: [54.5 ÷ 311.3] mm, according to the data provided by DSO.
- Gas consumption G_{ext} for each consumption point (including FRSs) in the range: [1.8 10^{-5} ÷ 0.19] kg/s, converted from the data provided by DSO.

The results of no blending scenarios are presented in Chapter 4 as a practical demonstration of the proposed methodology, along with a preliminary assessment of the opportunities and challenges offered by surrogate modelling. Subsequently, the methodology is extended to incorporate hydrogen injection scenarios.

In Chapter 5, the performance of the surrogate models generated through the application of ML techniques is assessed, and the results for e

ach hydrogen blending test case are discussed in detail.

The research leading to these results has received funding from Horizon 2020, the European Union's Framework Programme for Research and Innovation (H2020) under grant agreement n° 101111888.

4 Methodology

4.1 Modelling workflow and key method features

The proposed approach addresses the modeling of the parametric behavior of multiple output responses, such as fluid-dynamic quantities including pressure, velocity, and flow rate, in a gas network as functions of a common set of input parameters. The methodology is based on a ML vector-valued regression framework. Each input vector represents a set of design or geometrical parameters, while each output vector aggregates the system responses under consideration (e.g., the pressure values at all nodes of the network).

The regression model adopted in this work is KRR, enabling the modeling of nonlinear relationships between inputs and outputs while maintaining a convex and well-posed optimization problem. It is important to note that, in the class of problems considered (i.e., gas networks), the dimensionality of the output space is typically large, often in the order of several hundred. This feature makes the problem challenging and stresses the benefits of the proposed solution, which turns out to be particularly well suited for quality assessment tasks.

The detailed mathematical formulation of the model, along with complete modeling workflow, is described in Appendix A. In the following, the procedure is briefly summarized and split into the major steps, which are detailed further in the mentioned appendix.

(A) INITIALIZATION

The modeling task is set up by defining the solver settings, the input parameters, and the sizes of the datasets in terms of the overall number of Monte Carlo (MC) simulations using the steady-state gas-network solver. Each input parameter is characterized by a mean value and an associated variability range. Based on their statistical distributions, normalized samples of the input parameters are generated for both the training and test sets. A number `N_MC` of MC simulations using the gas-network solver are carried out for data collection (see next step). Among them, a subset of `N_ED` is randomly chosen as a training dataset. The remaining samples (`N_MC - N_ED`) will be used for surrogate model testing.

(B) DATA COLLECTION (TRAINING SET AND TEST SET)

For the training and test set, each normalized input sample is transformed into physical parameter values and used as input to the gas-network solver. When the simulation is successful, the resulting outputs (such as the node pressure) are stored to build the training database. The overall dataset is then randomly split into the training and test set. Optional post-processing of solver outputs may be applied in both cases.

(C) MODEL TRAINING

The collected training inputs and outputs are used to construct a vector-valued surrogate model using a custom implementation of the vector-valued KRR regression (see the Appendix). Model parameters and hyperparameters are identified during training.

(D) SURROGATE MODEL ACCURACY ASSESSMENT

The trained surrogate model is evaluated on the test input set. Model predictions are compared against the corresponding solver outputs using standard performance metrics and graphical tools, such as scatter plots, to assess accuracy and predictive reliability.

The research leading to these results has received funding from Horizon 2020, the European Union's Framework Programme for Research and Innovation (H2020) under grant agreement n° 101111888.

(E) STATISTICAL ANALYSIS

Once validated, the surrogate model is used to efficiently perform statistical analyses of the gas-network outputs. This includes studying the output mean, variability, trends, and sensitivities with respect to the input parameters, enabling deeper insight without further high-fidelity simulations.

In Figure 4-1 a flowchart summarizing the workflow described above is given

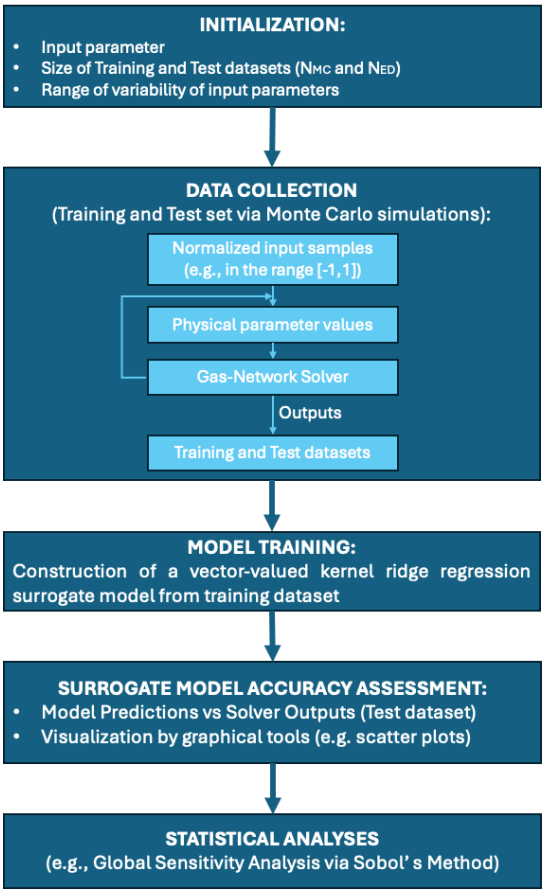

Figure 4-1: Flowchart of the generation of the surrogate model of the gas network and its utilization for statistical analysis.

4.2 4 input parameter test case

The parameters collected in the input vector $\boldsymbol{x}$ include:

1. Entry pressures at both ReMi stations (with a variation $\Delta P = \pm 7$ %);
2. Pipeline diameters ($\Delta D = \pm 5$ %);
3. Pipeline roughness ($\Delta E = \pm 10$ %);
4. Exit flow to Riccione users ($\Delta G_{ext} = \pm 20$ %). In the first application, this parameter affects all exit flows equally, causing them to vary by the same amount.

The research leading to these results has received funding from Horizon 2020, the European Union's Framework Programme for Research and Innovation (H2020) under grant agreement n° 101111888.

All parameter variations are assumed to be uniformly distributed around their nominal values. In addition, the variation in pipe diameters is introduced for illustrative purposes, to evaluate the feasibility of the proposed approach and to quantify the sensitivity of the results to individual parameters.

This initial network configuration and the selected set of parameters can be used to identify the most stressed sections of the infrastructure in terms of: (i) pressure (to remain within prescribed limits); (ii) flow rate (within allowable bounds); (iii) velocity (within safe operating limits).

To generate a sufficiently large dataset of network responses, `N_MC=2000` Monte Carlo simulations are performed using the open-source simulator, with the parameters randomly varied within their respective ranges. As briefly mentioned in the workflow, from the total set of simulations, a smaller subset is selected for model training (i.e., model generation). Specifically, the number of training samples `N_ED` is set to either 20 or 50 in this first illustrative example. A multi-output model is trained for each output class, i.e., the 241 pressures of each node for the first model, 249 pipe flowrates for the second model, and 249 velocities for the third model.

4.2.1 Machine Learning outcomes

Figure 4-2 presents the so-called scatter plots for the prediction of nodal pressure, one of the three output variables considered for this network. Each plot compares, for every node and for each parameter configuration in the test set, the reference network response with the corresponding surrogate model prediction. The closer the cloud of points lies to the bisector line, the better the model performance. From these results, it is evident that good accuracy can be achieved even with a small number of training samples. A few tens of samples are sufficient to reproduce the network behavior effectively. Similar trends are observed for the other output variables, namely flow rates and velocities (see **Figure 4-3**).

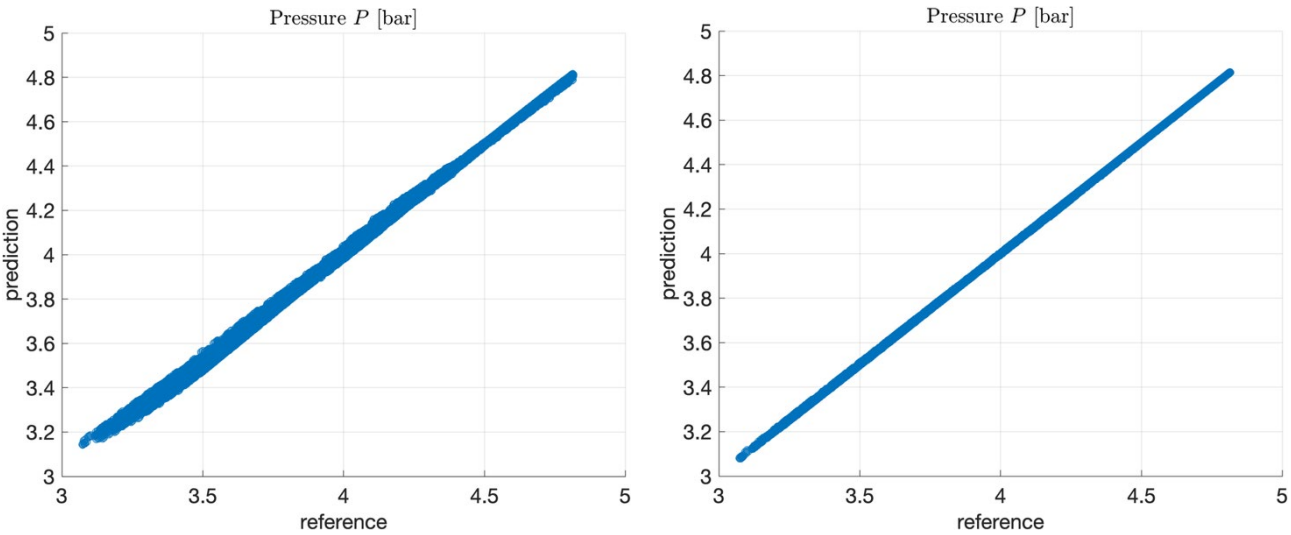

Figure 4-2: scatter plots showing the nodal pressure validation samples versus the corresponding KRR model predictions for all network nodes, obtained using different numbers of training samples (left: 20 training samples, right: 50 training samples).

The research leading to these results has received funding from Horizon 2020, the European Union's Framework Programme for Research and Innovation (H2020) under grant agreement n° 101111888.

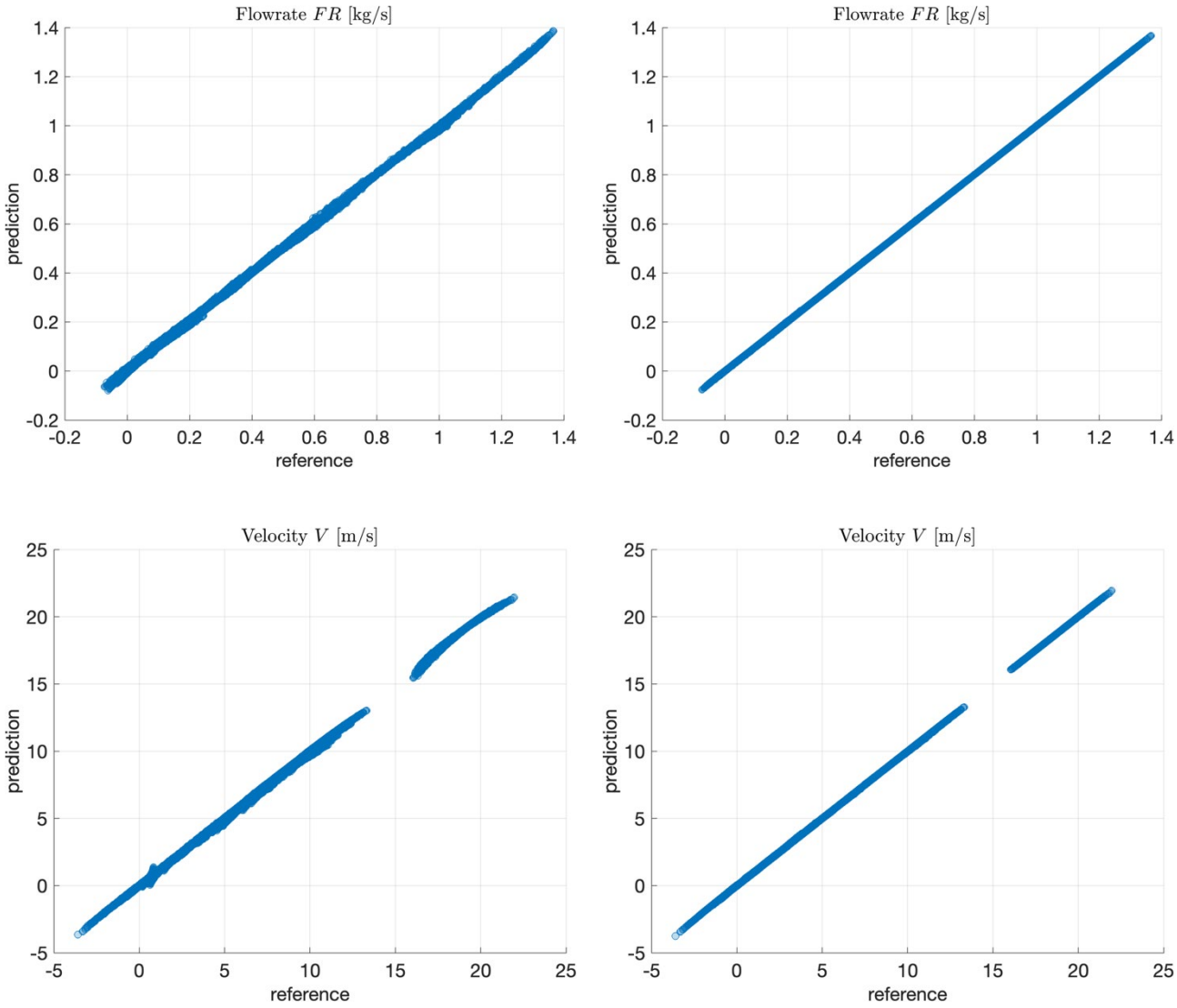

Figure 4-3: scatter plots showing the pipe flowrate (top) and gas velocity (bottom) validation samples versus the corresponding KRR model predictions for all network nodes, obtained using different numbers of training samples (left: 20 training samples, right: 50 training samples).

Note that the discontinuity in the data distribution along the bisector is due to unobserved values from the physical simulation: there are no pipelines displaying velocities within that range. Also, the negative values for mass flowrates and velocity are connected to the convention that has been used in identifying inlet and outlet nodes of each pipeline: when mass flows and velocities are negative it means that the conventional pipeline versus is, in fact, the opposite than the versus of the flux.

The research leading to these results has received funding from Horizon 2020, the European Union's Framework Programme for Research and Innovation (H2020) under grant agreement n° 101111888.

4.2.2 Surrogate model computational performances

The computational benefit of the proposed approach is noteworthy. Performing 2000 MC simulations with the physical model requires approximately 10 hours in total (about 19 s per run), whereas the corresponding surrogate model evaluations take 12.4 ms in total. The training of the vector-valued KRR model with 50 training samples, requires about 10.4 s. A single model is built once for each of the three considered output variables (i.e., the pressure, the flowrate and the velocity. All simulations were carried out on a MacBook Air equipped with an M3 processor and 24 GB of RAM. For a fair comparison, the total MC simulation time (10 h) should be contrasted with the sum of the training sample generation, model training and prediction CPU times, which amounts to approximately 15 minutes for 50 training samples, therefore yielding a substantial speed-up.

4.2.3 Surrogate model applicability

Once the model is generated and its accuracy verified, it can be effectively used to analyze specific operating conditions of the gas network or to easily and quickly analyze its performance over the considered parameter variations. A representative visualization is provided in Figure 4-4, which shows the layout of the Riccione distribution network along with the mean values and standard deviations of the nodal pressures. The standard deviation reflects the variability associated with parameter uncertainty and constitutes a fundamental statistical metric for quantifying the dispersion of data points around their mean value. Nodes highlighted in red correspond to areas where the impact of parameter variations is more significant. A similar visualization is presented in Figure 4-5 for the other two output variables, where analogous observations can be made. It should be emphasized that the plots in the above-mentioned two figures are produced from the predictions of the obtained surrogate model, for 2000 parameter configurations randomly selected within their specified ranges of variation.

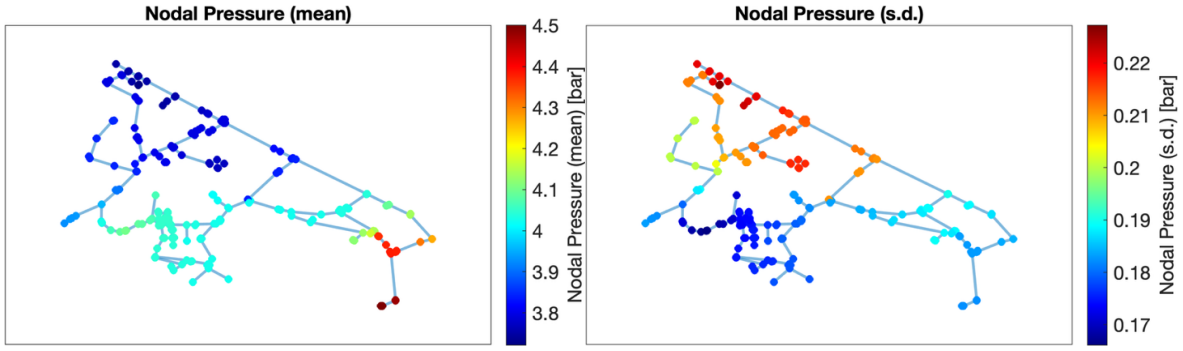

Figure 4-4: layout of the example Riccione distribution network along with the mean values and standard deviations of the nodal pressures.

The research leading to these results has received funding from Horizon 2020, the European Union's Framework Programme for Research and Innovation (H2020) under grant agreement n° 101111888.

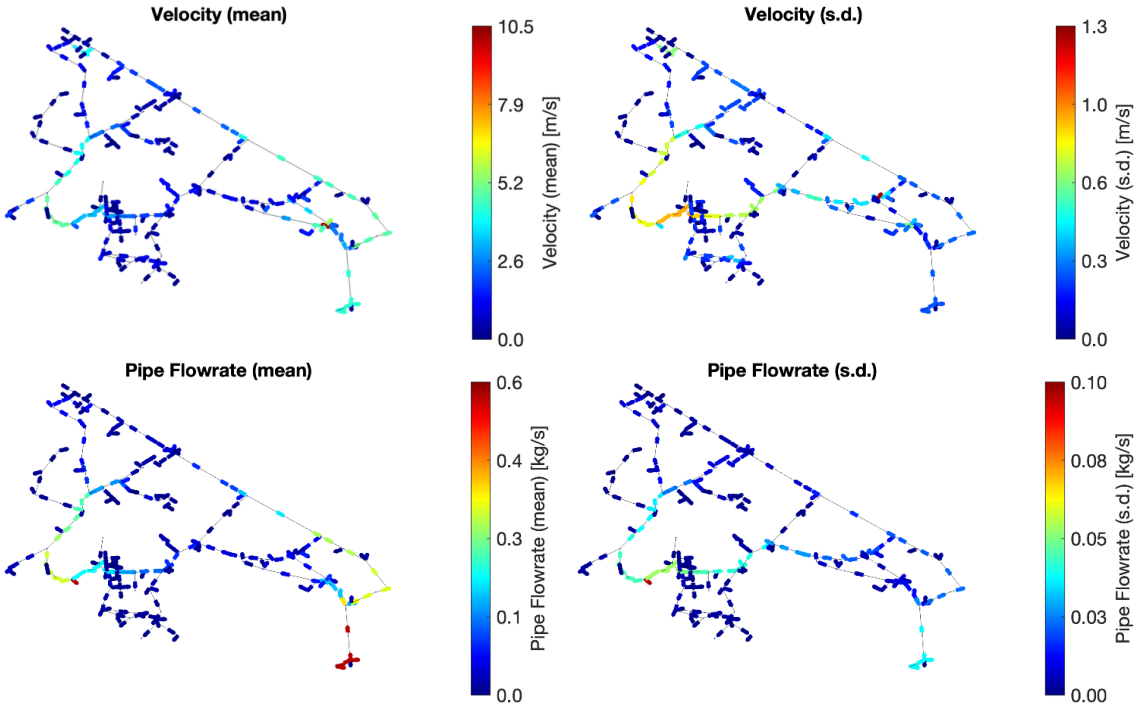

Figure 4-5: layout of the example Riccione distribution network along with the mean values and standard deviations of the pipe flowrates and velocity.

4.2.3.1 Global Sensitivity Analysis

We now leverage the surrogate models to perform a global sensitivity analysis aimed at quantifying the impact of each individual input parameter on the variability of the outputs. This assessment proves particularly valuable for identifying potentially critical zones within the network, where certain parameters exert a stronger influence and may lead to significant variations in key quantities of interest, such as pressures in this initial example, and, more importantly, hydrogen concentrations in the subsequent test cases presented in the application chapter (chapter 5).

Specifically, we apply the so-called Sobol' method, a variance-based sensitivity analysis which decomposes the output variance into components that can be attributed to each input parameter considered separately.

The total-effect Sobol' indices are computed as

$$S_{T_i} = \frac{\mathrm{E}_{\boldsymbol{X}_{\sim i}}\left(\mathrm{Var}_{X_i}(Y|\boldsymbol{X}_{\sim i})\right)}{\mathrm{Var}(Y)}$$

and measure the contribution of the i-th input x_i to the output variance, including also all interactions with other input parameters. In the above formula, $\mathrm{Var}(Y)$ denotes the total variance of the output y and $Y|\boldsymbol{X}_{\sim i}$ denotes the output y computed by fixing all inputs except x_i to a constant value. Hence, $\mathrm{E}_{\boldsymbol{X}_{\sim i}}\left(\mathrm{Var}_{X_i}(Y|\boldsymbol{X}_{\sim i})\right)$ is the expectation of the variances over x_i computed by fixing the other inputs to a constant (though random) value.

In practice, the above moments cannot be computed analytically, but they are rather estimated using quasi-Monte Carlo methods. One common approach to improve the efficiency of the estimators is to generate a suitable low-discrepancy sequence of points, such as the Sobol' sequence. The procedure is described as follows:

The research leading to these results has received funding from Horizon 2020, the European Union's Framework Programme for Research and Innovation (H2020) under grant agreement n° 101111888.

1. Generate a $N \times 2p$ sample matrix, where p is the number of input parameters, using a Sobol' sequence with N points in the $2p$-dimensional hyperspace and with the same distribution as the input variables.
2. Form two distinct sets of samples, $\boldsymbol{A}$ and $\boldsymbol{B}$, using the first and last d columns of the sample matrix.
3. Build p matrices $\boldsymbol{A}_B^i$, of size $N \times p$, with $i = 1, \dots, p$, such that the i-th column is from matrix $\boldsymbol{B}$, whereas the remaining columns are from matrix $\boldsymbol{A}$.
4. Estimate the numerator of S_{T_i} as

$$E_{\boldsymbol{X}_{\sim i}}\left(\mathrm{Var}_{X_i}(Y|\boldsymbol{X}_{\sim i})\right) \approx \frac{1}{2N}\sum_{j=1}^{N}\left(f(\boldsymbol{A})_j - f\left(\boldsymbol{A}_B^i\right)_j\right)^2$$

where $f(\boldsymbol{A})_j$ and $f\left(\boldsymbol{A}_B^i\right)_j$ denote the model evaluated for the j-th sample of set $\boldsymbol{A}$ and $\boldsymbol{A}_B^i$, respectively.

The length N of the sequence defines the accuracy of the estimator. Typical values are on the order of $N \sim 10^3$ or 10^4. In total, $N(d+1)$ model evaluations are required for the dataset $\boldsymbol{A}$ and each of the d datasets $\boldsymbol{A}_B^i$, all of length N. Therefore, this calculation is hardly feasible with the original computational model, but it can be carried out at negligible cost using the ML surrogate.

As an application example, we focus the sensitivity analysis on the nodes exhibiting the largest variance of the nodal pressure and flow velocity. As shown in Figure 4-6, there are three separate clusters of nodes with a pressure standard deviation that is significantly above 0.2 bar. These correspond to peripheral nodes away from the inlets. We select one node for each cluster for the sensitivity analysis, namely nodes 7, 80, and 229.

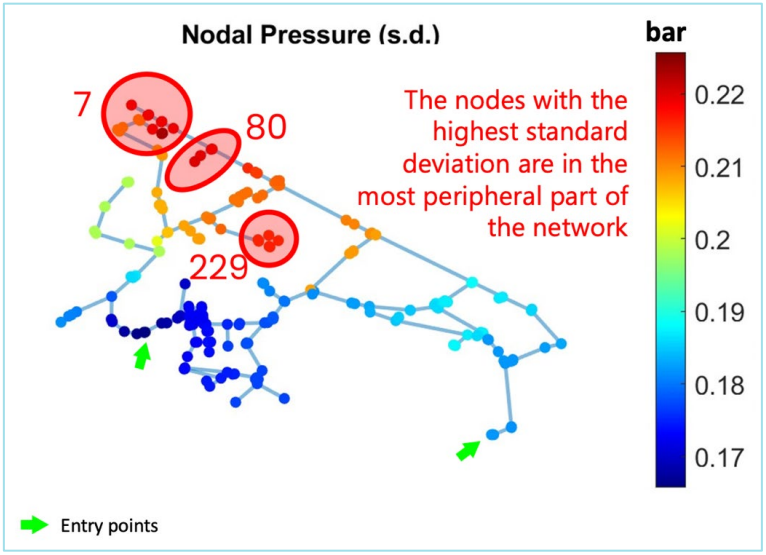

Figure 4-6: variance of nodal pressure. The three clusters highlighted in red in the top-left corner of the network exhibit the largest variance on the nodal pressure.

Figure 4-7 shows the total-effect Sobol' indices for the nodal pressure and for each of the four input parameters, i.e., pipe diameter, inlet pressure, pipe roughness, and consumption. A similar effect is observed for all the three nodes, with the largest contribution from the inlet pressure, followed by consumption and the pipe diameter. A negligible effect is established for the pipe roughness.

The research leading to these results has received funding from Horizon 2020, the European Union's Framework Programme for Research and Innovation (H2020) under grant agreement n° 101111888.

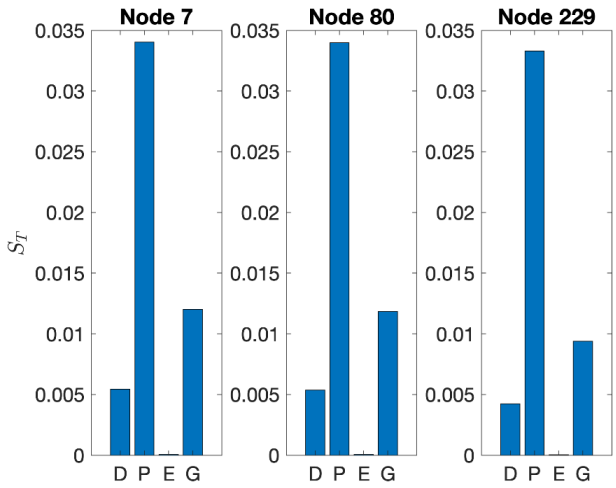

Figure 4-7: total-effect Sobol' indices for the pressure on the three selected nodes (7, 80, and 229) highlighting the individual contribution of the pipe diameter (D), inlet pressure (P), pipe roughness (E), and consumption (G). A similar effect is observed for all the three nodes, with the largest and smallest impact from the entry pressure and pipe roughness, respectively.

Similarly, for the sensitivity analysis of the flow velocity, we focus on the three clusters exhibiting the largest standard deviation, exceeding 0.8 m/s as highlighted in **Figure 4-8**. These correspond to locations where network loops join. We select one edge from each cluster, namely edges 84, 186, and 240. **Figure 4-9** shows the sensitivity analysis for the branch velocity. Again, the individual contribution of the input parameters is similar for each branch. However, the largest effect is in this case from the consumption, while the pipe roughness still plays a negligible role.

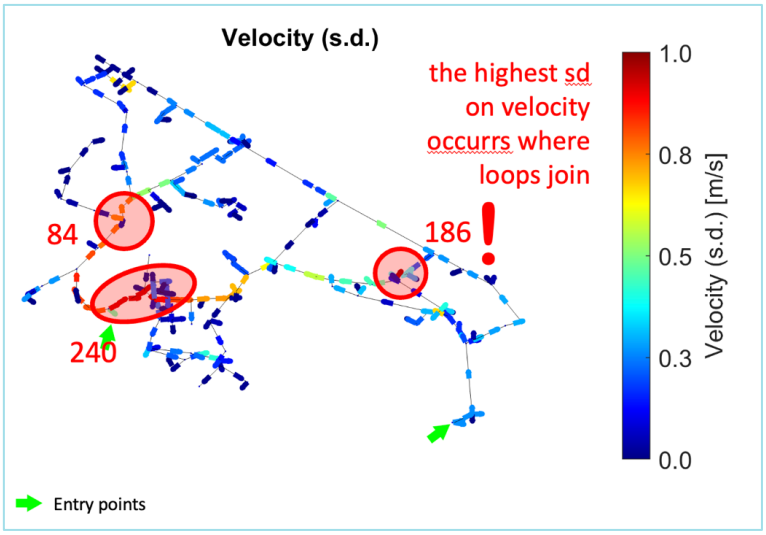

Figure 4-8: variance of flow velocity. The three clusters highlighted in red exhibit the largest variance on the flow velocity.

…

The research leading to these results has received funding from Horizon 2020, the European Union's Framework Programme for Research and Innovation (H2020) under grant agreement n° 101111888.

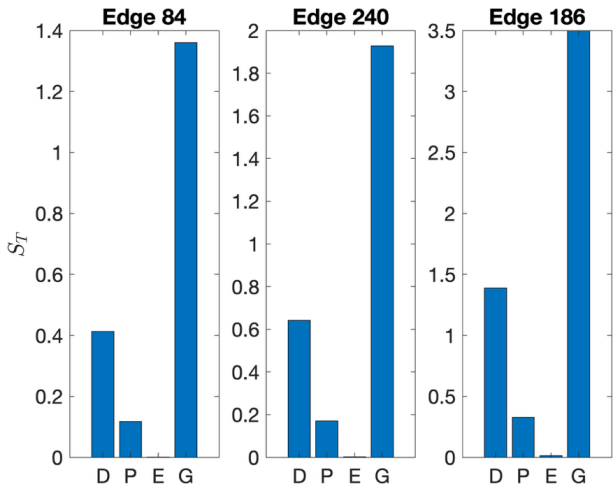

Figure 4-9: total-effect Sobol' indices for the velocity on the three selected branches (84, 186, and 240). Also in this case, the effect is similar for each branch, but the largest contribution is now from the consumption.

It is worth emphasizing that, for larger networks involving multiple varying parameters, the proposed statistical framework enables the DSO to identify the most critical points of the network in advance. This facilitates more effective monitoring and proactive management of the infrastructure.

4.3 29 input parameters test case - results

In this second example, the method is stressed by increasing the number of independent parameters from 4 to 29. Specifically, the single parameter P considered above and controlling both input pressures is replaced by two separate parameters accounting for the entry pressures at the Primary and Secondary ReMi stations, meaning that the variation of pressures at the inlet points are not correlated. Likewise, instead of applying the same variation to all exit flows through a single parameter G_{ext}, 25 exit flows are varied independently. To sum up:

- Par.1) Entry pressures at ReMi station 1 (with a variation $\Delta P = \pm 7$ %);
- Par 2) Entry pressures at ReMi station 2 (with a variation $\Delta P = \pm 7$ %);
- Par.3) Pipeline diameters ($\Delta D = \pm 5$ %);
- Par.4) Pipeline roughness ($\Delta E = \pm 10$ %);
- Par.5-29) Exit flow to Riccione clusters of users ($\Delta G_{ext} = \pm 20$ %): each cluster is represented by one final reduction station plus a cluster composed by all the users directly connected to the higher-pressure tier.

Figure 4-10 presents the scatter plots for the nodal pressures obtained with an increasing number of training samples, ranging from 20 to 300. From these results, it can be observed that the model accuracy improves as the number of training samples increases. A similar behaviour is observed for the other two output variables, as shown in Figure 4-11 and Figure 4-12.

The research leading to these results has received funding from Horizon 2020, the European Union's Framework Programme for Research and Innovation (H2020) under grant agreement n° 101111888.

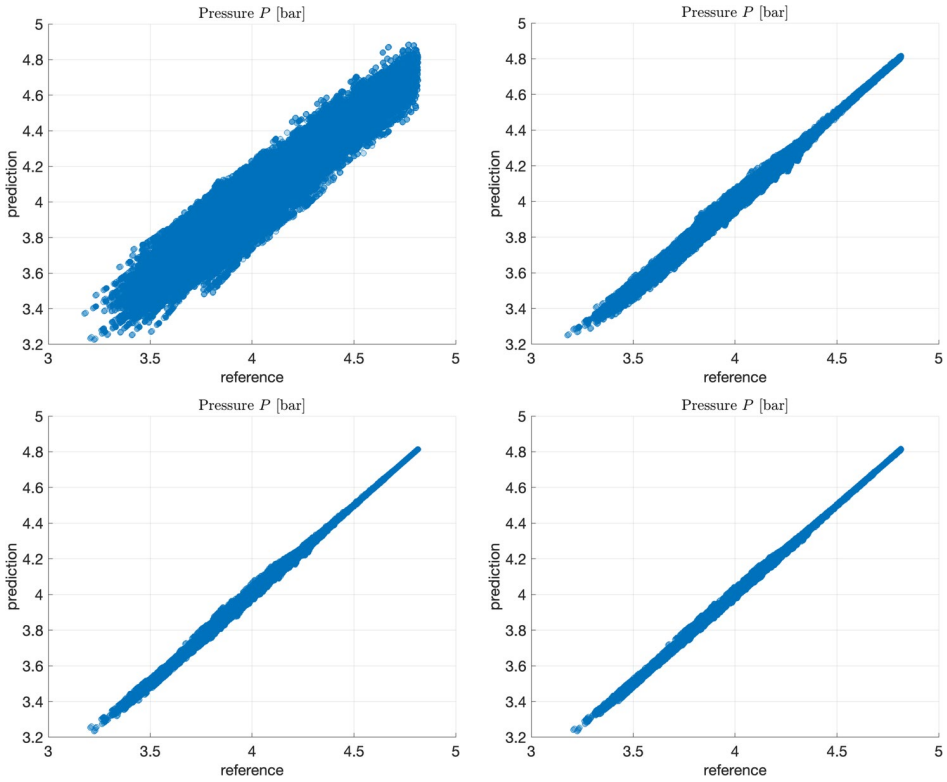

Figure 4-10: scatter plots comparing the nodal pressure validation samples versus the corresponding KRR model predictions for all network nodes, obtained using different numbers of training samples (top left: 20, top right: 50, bottom left: 150, bottom right: 300).

The research leading to these results has received funding from Horizon 2020, the European Union's Framework Programme for Research and Innovation (H2020) under grant agreement n° 101111888.

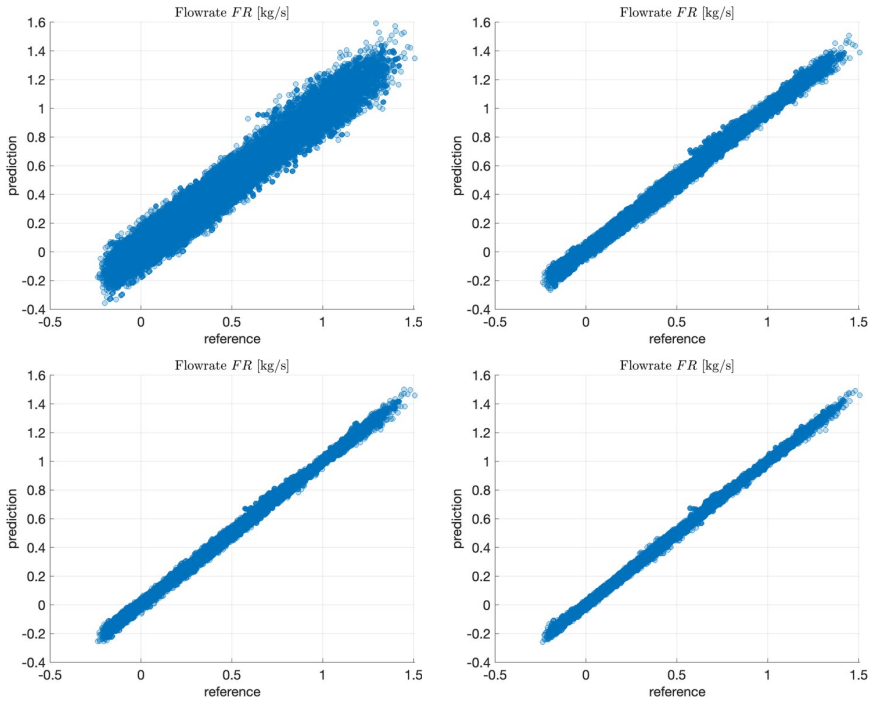

Figure 4-11: Scatter plots comparing the pipe flowrate validation samples versus the corresponding KRR model predictions for all network nodes, obtained using different numbers of training samples (top left: 20, top right: 50, bottom left: 150, bottom right: 300).

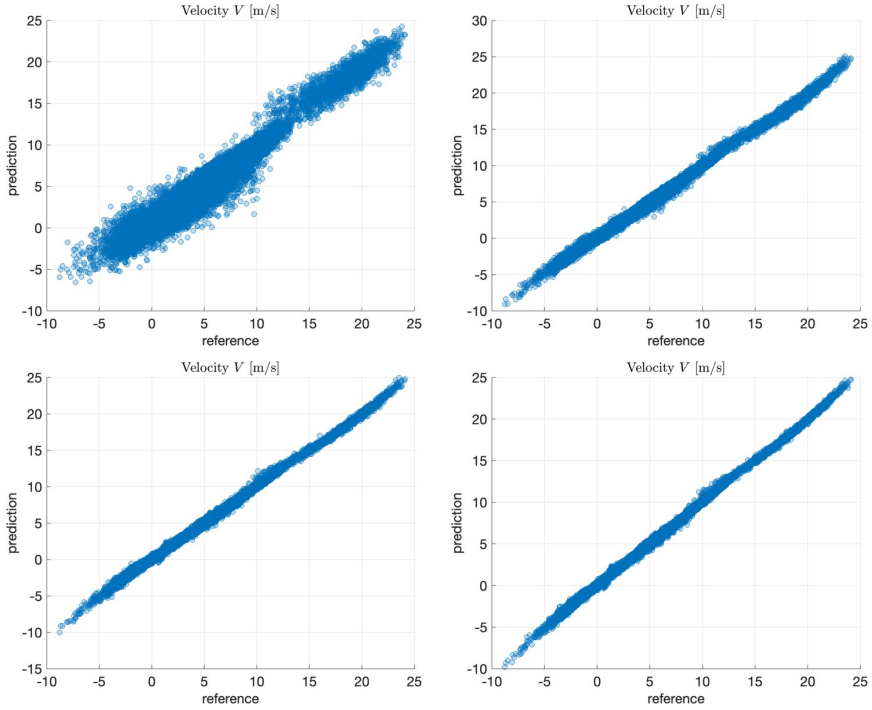

Figure 4-12: Scatter plots comparing the velocity validation samples versus the corresponding KRR model predictions for all network nodes, obtained using different numbers of training samples (top left: 20, top right: 50, bottom left: 150, bottom right: 300).

The research leading to these results has received funding from Horizon 2020, the European Union's Framework Programme for Research and Innovation (H2020) under grant agreement n° 101111888.

This comparison was intended to assess the robustness of the proposed surrogate modelling approach, which demonstrates a remarkable prediction accuracy even when handling a larger number of input parameters, though naturally requiring a larger number of training samples.

4.4 Extension to Hydrogen Blending cases

Following a direct physical interpretation, the quality mixing module can be readily formulated as a simple weighted average of the gas compositions entering each node, as detailed in this section (with the weights being the entering flow rates). It can be regarded as an additional, lightweight (i.e., superfast) module that relies on the known network topology and on the ML-based models previously developed to predict fluid-dynamic variables. More specifically, the pipeline flowrates FR and the nodal gas exchanges G_{ext} are the needed fluid-dynamic quantities. Thus, together with the ML model for the flowrates FR, an additional ML model for the nodal gas exchanges G_{ext} is also built. The methodology is illustrated in Figure 4-13: the Monte Carlo simulations are run using the steady state physical model with the quality mixing loop: this gas quality sensitive section acts as a further iterative procedure that allow to accounts for the gas quality impact on the fluid-dynamics of the network. The steady state result is reached when both the fluid-dynamic and the quality mixing iterative loops has converged. Under the gas quality point of view, the solution represents the network configuration with the gas mixing fully developed throughout the network. Thus, the resulting flowrates FR and the nodal gas exchanges G_{ext} accounts for the local gas quality. So, the surrogate models which will be trained for predicting FR and G_{ext} are trained over the results from the overall physical model (including the concentration loop) so that the fluid-dynamic quantities are influenced by the gas quality.

The quality mixing equation is explained hereafter, for the sake of clarity.

Under a perfect mixing assumption, the mixing module of the fluid-dynamic model applies, for each node, the following formula:

$$\left[w_{(c)}\right]_{i^*} = \frac{-\sum_j a^-_{i^*,j}\,\dot{m}_j \cdot \left[w_{(c)}\right]_j - \dot{m}^{(-)}{}_{ext_{i^*}} \cdot \left[w_{(c)}\right]_{ext_{i^*}}}{\sum_j a^+_{i^*,j}\,\dot{m}_j + \dot{m}^{(+)}{}_{ext_{i^*}}}$$

where: $$a^+_{i^*,j} = \begin{cases} +1, & \text{pipe } j \text{ is outgoing from junction node } i^* \\ 0, & \text{pipe } j \text{ is incoming to junction node } i^* \\ 0, & \text{pipe } j \text{ has no connections with junction node } i^* \end{cases}$$

$\dot{m}^{(+)}{}_{ext_{i^*}}$ is the withdrawn gas flow from junction node i^*; in the specific case study, this term will be different from zero where gas consumption is located (mainly at the gas reducing stations).

$$a^-_{i^*,j} = \begin{cases} 0, & \text{pipe } j \text{ is outgoing from junction node } i^* \\ -1, & \text{pipe } j \text{ is incoming to junction node } i^* \\ 0, & \text{pipe } j \text{ has no connections with junction node } i^* \end{cases}$$

$\dot{m}^{(-)}{}_{ext_{i^*}}$ is the injected gas flow in junction node i^*; in the specific case study, this term will be different from zero where gas enters the network (thus at the ReMi stations).

And:

$\left[w_{(c)}\right]_{i^*}$ is the mass fraction of the component c at the junction node i^*; it is the unknown of the equation, resulting from the perfect mixing of the incoming fluxes.

The research leading to these results has received funding from Horizon 2020, the European Union's Framework Programme for Research and Innovation (H2020) under grant agreement n° 101111888.

$[w_{(c)}]_j$ is the mass fraction of the component c at all the adjoining nodes that are connected to the junction node i^* through the j^{th} pipe.

$[w_{(c)}]_{ext_{i^*}}$ is the mass fraction of the component c within the mass flux that is injected from outside in the network.

The mass fractions can then be converted into molar fractions, more commonly used in the framework of gas quality tracking and management.

The needed fluid-dynamic variables to extend any ML surrogate model to the hydrogen blending and quality monitoring case are:

$$G_{ext} \rightarrow vector\ of\ all\ the\ \dot{m}_{ext_i}\ (for\ all\ the\ nodes)$$

$$FR \rightarrow vector\ of\ all\ the\ \dot{m}_j\ (for\ all\ the\ pipes)$$

To be noted that concerning the surrogate model prediction of G_{ext}, only the flowrates exchanged at the nodes where the pressure is set (in this case at the Remi Stations) are indeed predictions. All the others are independent variables.

The following flow diagram (Figure 4-13) shows the rationale of this methodology.

The research leading to these results has received funding from Horizon 2020, the European Union's Framework Programme for Research and Innovation (H2020) under grant agreement n° 101111888.

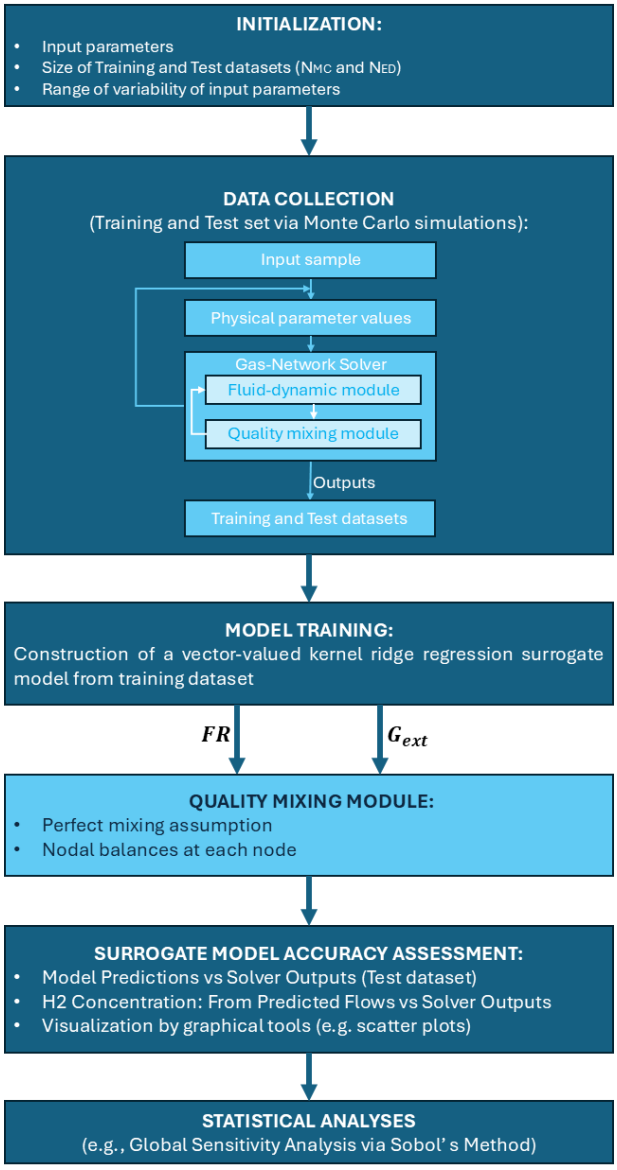

Figure 4-13: Flowchart of the generation of the surrogate model of the gas network in the case of hydrogen blending simulations.

The research leading to these results has received funding from Horizon 2020, the European Union's Framework Programme for Research and Innovation (H2020) under grant agreement n° 101111888.

5 Application Cases with H_2 blending – Results and Discussion

The following test cases have been considered regarding hydrogen blending:

a) 4 input parameters with one hydrogen injection:
- Par.1) Entry pressures at both ReMi stations (with a variation $\Delta P = \pm 7$ %);
- Par.2) H2 blending at the primary ReMi station ($10\% \pm \Delta H = \pm 95$ %);
- Par.3) Pipeline roughness ($\Delta E = \pm 10$ %);
- Par.4) Exit flow to Riccione users ($\Delta G_{ext} = \pm 20$ %).

b) 5 input parameters with two hydrogen injection:
- Par.1) Entry pressures at both ReMi stations (with a variation $\Delta P = \pm 7$ %);
- Par.2) H2 blending at the primary ReMi station ($10\% \pm \Delta H = \pm 95$ %);
- Par.3) H2 blending at the secondary ReMi station ($10\% \pm \Delta H = \pm 95$ %)
- Par.4) Pipeline roughness ($\Delta E = \pm 10$ %);
- Par.5) Exit flow to Riccione users ($\Delta G_{ext} = \pm 20$ %).

c) 30 input parameters test case with two hydrogen injection:
- Par.1) Entry pressures at ReMi station 1 (with a variation $\Delta P = \pm 7$ %);
- Par 2) Entry pressures at ReMi station 2 (with a variation $\Delta P = \pm 7$ %);
- Par.3) H2 blending at the primary ReMi station ($10\% \pm \Delta H = \pm 95$ %);
- Par.4) H2 blending at the secondary ReMi station ($10\% \pm \Delta H = \pm 95$ %)
- Par.5) Pipeline roughness ($\Delta E = \pm 10$ %);
- Par.6-30) Exit flow to Riccione clusters of users ($\Delta G_{ext} = \pm 20$ %).

In the following section, the ML outcomes for each blending case is given. The only input that is related to the network's hardware is the roughness, which is usually an unknown parameter, and it is assumed depending on the material of the pipe and, possibly, its age. The variations of the diameters have been omitted, since are well-defined design parameters determined during construction and are not subject to significant variation, especially in analyses oriented towards operational strategy and network management.

5.1 Machine Learning outcomes

The described ML methodology has been applied to each case allowing to generate a surrogate model for each of the following variables:

- $P \rightarrow$ nodal pressures;
- $FR \rightarrow$ pipeline mass flow rates;
- $G_{ext} \rightarrow$ nodal mass flow exchanged with the external environment (injections and consumptions)
- $V \rightarrow$ pipeline gas velocity;

In the following subsections, the scatter plots of FR and G_{ext} (which are the relevant variables to the quality mixing problem) are given together with the one of the nodal hydrogen concentrations to show the performance of the surrogate models.

5.1.1 4 input parameters with one hydrogen injection

Dataset of network responses: `N_MC=500;`
Training samples (randomly chosen among the dataset of `N_MC`): `N_ED=200;`

The research leading to these results has received funding from Horizon 2020, the European Union's Framework Programme for Research and Innovation (H2020) under grant agreement n° 101111888.

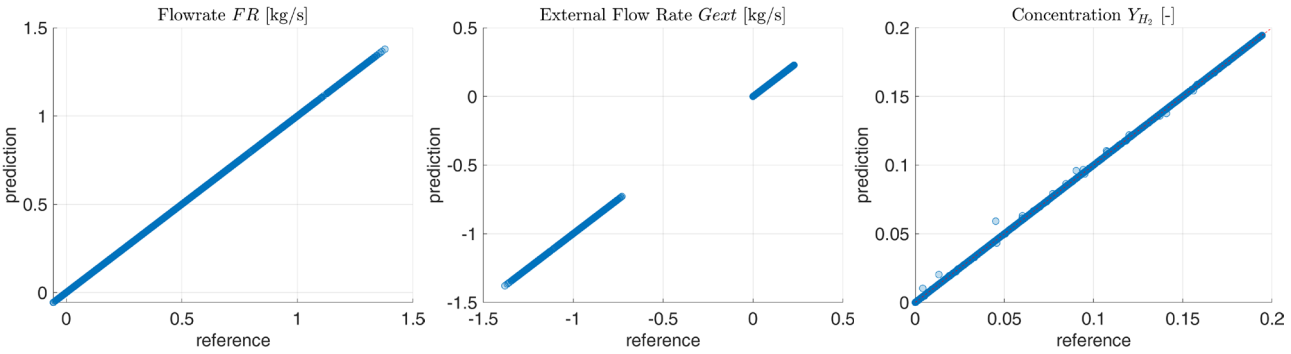

Figure 5-1: Scatter plots for the validation of the surrogate models relevant for the hydrogen injection case (4 parameters, 1 H_2 injection). From left to right: pipeline flow rate, nodal gas flows, nodal hydrogen concentrations.

Figure 5-1 displays the very good behaviour of the ML surrogate models of pipeline flow rates FR and nodal gas exchanges G_{ext} Note that the negative values represent all the possible injection flow rates which are calculated at the two gas entry points. By using the surrogate model predicted values FR and G_{ext} into the quality mixing formula explained in Section 4.4, the prediction of the hydrogen concentration is obtained. The scatter plot of the nodal concentration of shows a very strong alignment between predicted and reference values. This indicates that this surrogate model accurately represents the specific gas infrastructure configuration with hydrogen blending at one of the two injection points, across the entire range of parameter variations considered.

5.1.2 5 input parameters with two hydrogen injections

This case represents an extension of the previous one, in which hydrogen blends enter the network form both the entry points and the hydrogen shares can be set independently. Figure 5-2 shows that even adding an input parameter (i.e. the further hydrogen injection with a wide range of variation) the surrogate model can well represent the case. To be noted that the dataset size and the training samples are the same as the previous case.

Dataset of network responses: `N_MC=500;`
Training samples (randomly chosen among the dataset of `N_MC`): `N_ED=200;`

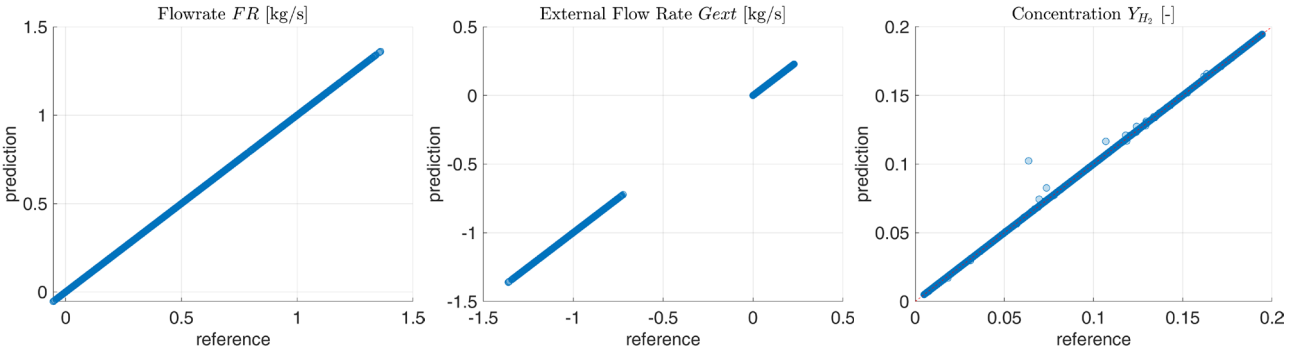

Figure 5-2: Scatter plots for the validation of the surrogate models relevant for the hydrogen injection case (5 parameters, 2 H_2 injections). From left to right: pipeline flow rate, nodal gas flows, nodal hydrogen concentrations.

The research leading to these results has received funding from Horizon 2020, the European Union's Framework Programme for Research and Innovation (H2020) under grant agreement n° 101111888.

5.1.3 30 input parameters with two hydrogen injections

In this case, the test is further expanded by allowing the independent variation of the pressure set points and the independent variation of 25 cluster of consumptions. This means testing the gas infrastructure on a very wide and general range of operating conditions, part of them which might be out of the usual operating domain. This variability explains the need to increase the size of the dataset of network responses with respect to the previous cases. Following the results obtained for the 29 parameters described in 4.3, the number of training samples has been chosen accordingly.

Dataset of network responses: `N_MC=1000;`
Training samples: `N_ED=400;`

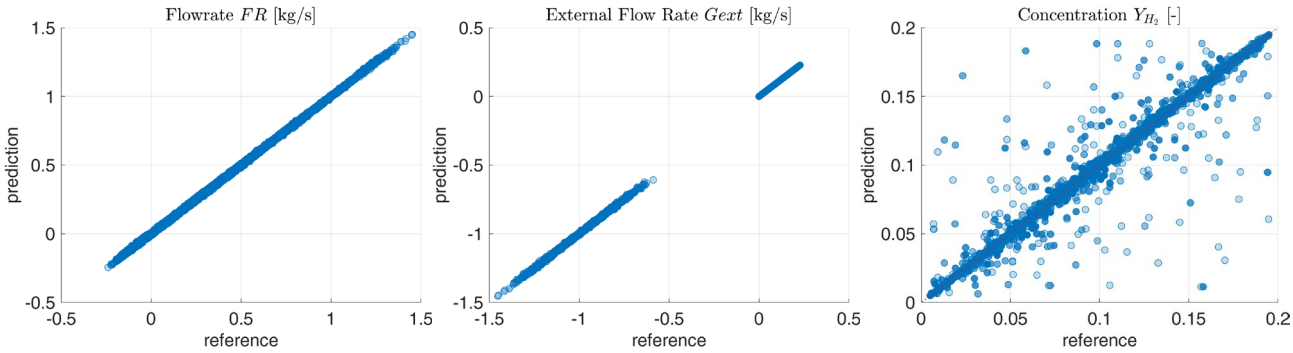

Figure 5-3: Scatter plots for the validation of the surrogate models relevant for the hydrogen injection case (30 parameters, 2 H_2 injections). From left to right: pipeline flow rate, nodal gas flows, nodal hydrogen concentrations.

The scatter plots in Figure 5-3 shows that on the fluid-dynamic side (FR and G_{ext} outputs) the predictions are still well aligned with the reference values form the physical model With regard to the scatter plot of the nodal hydrogen concentrations across all nodes, most samples lie close to the bisector, indicating good overall agreement. A limited number of points, however, show deviations. As will be demonstrated hereafter in this section, these discrepancies have a negligible impact on the key statistical metrics associated with hydrogen concentration. Therefore, further attempts to narrow the prediction band would provide limited practical benefit, particularly considering the objective of maintaining the training dataset within a relatively moderate size (on the order of a few hundred samples). The chosen metric to evaluate the quality of predictions of the hydrogen concentration at a given node is the Root Mean Square Error (RMSE), which is calculated as follows:

$$RMSE_i = \sqrt{\frac{1}{n}\sum_{k=1}^{n}\left(\hat{y}_{i,k} - y_{i,k}\right)^2}$$

where $\hat{y}_{i,k}$ is the predicted hydrogen concentration value in the i^{th} node for the k^{th} test sample and $y_{i,k}$ is the corresponding reference value (obtained by means of the physical model). $RMSE_i$ is then the value calculated for the node i over the whole validation samples n.

The left panel of Figure 5-4 shows the spatial distribution of the RMSE of the hydrogen concentration for each node in the network. The prediction error is not uniformly distributed but rather localized in specific areas. From a topological perspective, these areas correspond to the connections between network loops. Among the nodes exhibiting the highest errors—whose RMSE values remain below approximately 1%—the error appears to be distributed relatively evenly within subclusters, gradually increasing toward the small number of nodes where the maximum error is observed.

The research leading to these results has received funding from Horizon 2020, the European Union's Framework Programme for Research and Innovation (H2020) under grant agreement n° 101111888.

The magnitude of the RMSE remains small compared to the range of hydrogen concentration values, which vary between 0.5% and 19.5%. The plot in the right panel of the figure illustrates the distribution of the RMSE across the network nodes, showing that approximately only 20 out of 241 nodes exhibit an RMSE greater than 0.5%.

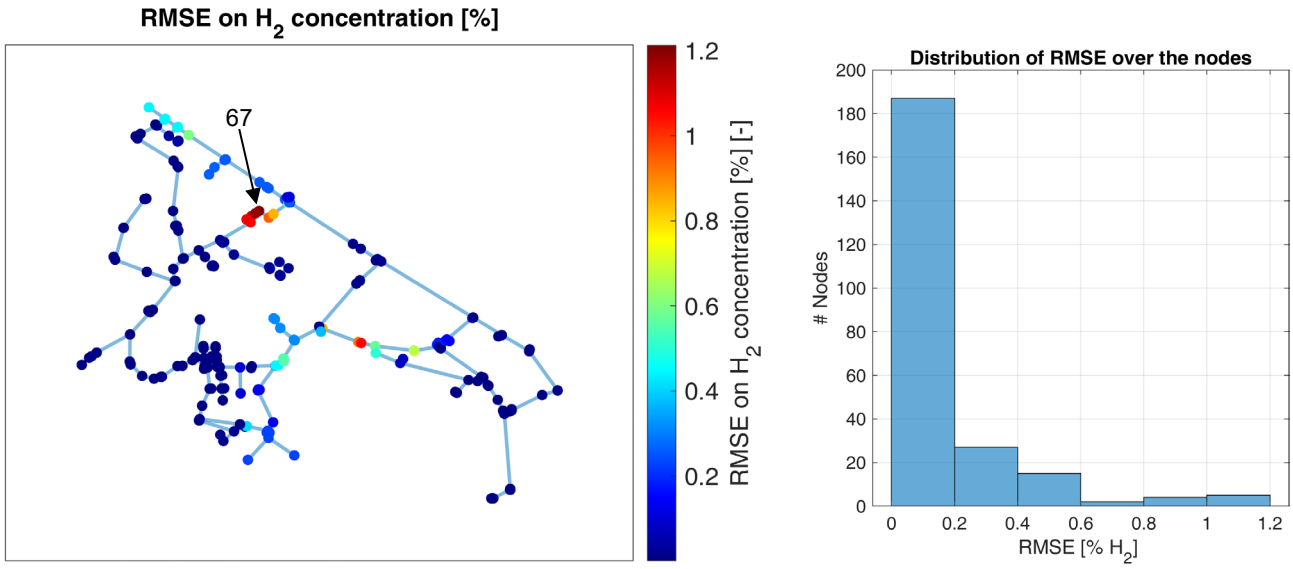

Figure 5-4: Left: network wide visualization of the RMSE on the nodal hydrogen concentration [%]; right: distribution of the RMSE over the network node.

For a deeper analysis, the node with the maximum value of RMSE has been addressed. The absolute error between prediction and reference has been evaluated for all the n validation samples. The normalized distribution is given in Figure 5-5 (left), showing that the frequency of the highest errors is negligible, thus it is possible to consider them as outliers.

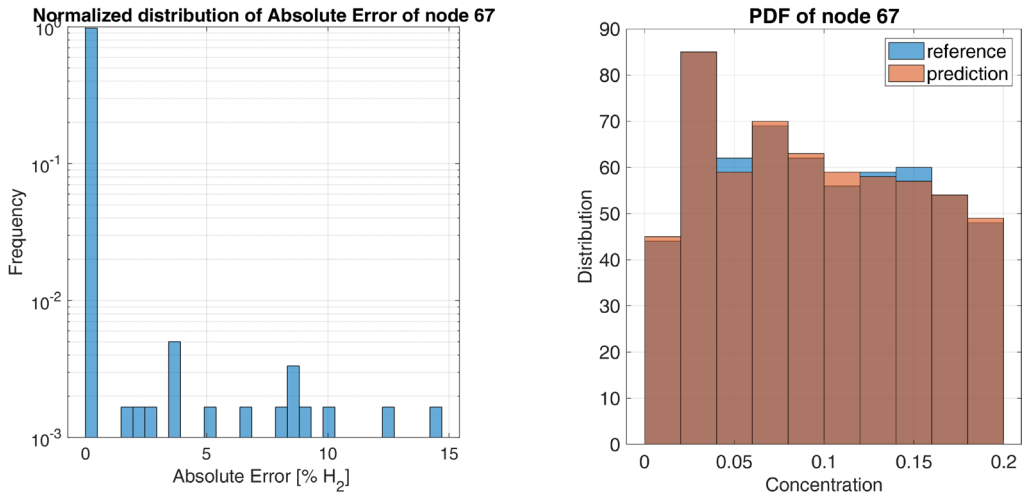

Figure 5-5: Left: normalized distribution of the absolute errors obtained for all the n validation samples for node 67, the one having the highest RMSE. Right: comparison between probability density functions (PDF) of the reference hydrogen concentration calculated in node 67 and the prediction ones.

The research leading to these results has received funding from Horizon 2020, the European Union's Framework Programme for Research and Innovation (H2020) under grant agreement n° 101111888.

Figure 5-5 (right) shows the comparison (by overlapping) of the probability density function of the hydrogen concentrations calculated in node 67 by the physical model (reference) and the one resulting from the surrogate model prediction, showing that the surrogate model has a very good prediction. In other words, this latter comparison highlights the negligible impact of a small number of points lying off the diagonal of the scatter plot in Figure 5-3.

The surrogate model is thus considered sufficiently accurate also for this test case.

5.2 Application Case Results: parametric and out-of-domain analysis

In the previous section, the surrogate models were tested and validated across three network scenarios involving hydrogen blending. The analysis was primarily limited to accuracy assessment, with particular emphasis on verifying that the models reliably predict both the fluid-dynamic variables and the hydrogen concentration.

In this section, the analysis is showcased to an application-oriented scenario, providing network operators with a tool enabling an in-depth investigation of network behavior and paving the way for out-of-domain generalization of the results. In other words, the models are employed to identify trends and effects of varying key parameters on network behavior in general and in particular focusing on the way hydrogen is spread throughout the network.

The hydrogen blending application cases have been presented in section 3.2. It is important to highlight that one surrogate model is built for each of the three application cases because the type and number of parameters change. The application cases are presented following an increased degree of complexity and generalization.

5.2.1 4 input parameters with one hydrogen injection

This scenario is representative of a distribution network where one of the two gas entry points is characterized by hydrogen blending (node 240). The blending may come from the upper level of the network (e.g. the gas entry point connected to a portion of the transmission network where hydrogen blending is present while the other is connected to another portion of the transmission network where only natural gas is present) or from hydrogen injection at the gas reduction station. In this case, as it was presented in section 3.2, the surrogate model has been trained over a uniform distribution of hydrogen blending centered in $10\%_{mol}$ and with a relative variation ±95% thus covering the range $[0.5\%_{mol} \div 19.5\%_{mol}]$. Thus, the resulting surrogate model is proved to be effective in covering this wide variability of the hydrogen blending.

Concerning the other parameters, the pressure set points at the two gas entry stations are changed simultaneously within a ±7% range around their respective set point. In Table 2 the pressure data are summarized:

Table 2: summary of the range of variation of the pressure parameter.

Inlet Node	Nominal pressure [bar_g]	Variation	Range [bar_g]
240	4.5	±7%	[4.185 ÷ 4.8],
241	4.1	±7%	[3.977 ÷ 4.387],

The research leading to these results has received funding from Horizon 2020, the European Union's Framework Programme for Research and Innovation (H2020) under grant agreement n° 101111888.

Given that the variation of the pressure set-points is governed by one single parameter, the ratio between the two inlet pressure values is constant under the possible configurations (rigid pressure set-point variation) , thus node 240 will always be the node set at the highest pressure.

The last variation parameter is the gas consumption throughout the network. A variation of $\pm 20\%$ is applied simultaneously to all the consumption nodes. This means that the consumption of all the users is rigidly translated throughout the domain of variation. This assumption is representative of a gas network where the behaviour of the user is quite homogeneous both in the temporal evolution and it is insensitive to the specific location on the network.

5.2.1.1 Concentration distribution

Some first general considerations can be drawn from the analysis of hydrogen concentration over the whole investigated domain. First, the nodal hydrogen concentration averaged over all the input parameter combinations uniformly distributed through the above-mentioned domain is analyzed together with the related standard deviation[3]

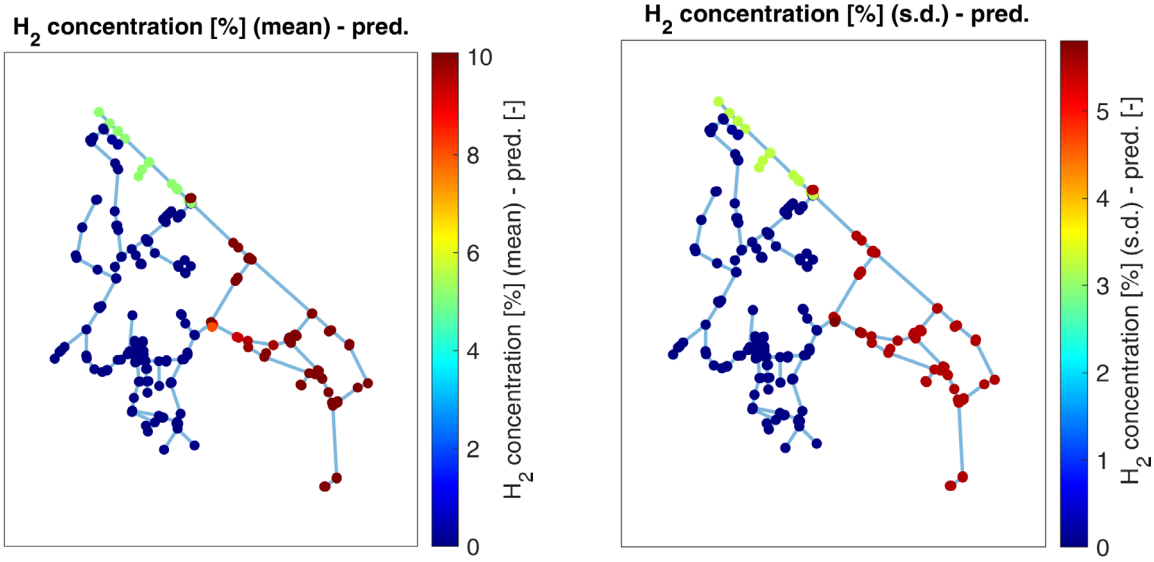

Figure 5-6: left: nodal hydrogen concentration as obtained from the surrogate model averaged over the whole parametric domain; right: corresponding standard deviation.

From the graph of the average hydrogen concentration (left in Figure 5-6) it is possible to draw that over all the pressure set-point range and the gas consumption variations (and over all the internal roughness ranges), the network displays three well distinct gas quality areas and a fourth "transitional" area where average concentration seems slightly less than $10\%_{mol}$. Intersecting this information with the one provided by the standard deviation (graph on the right) one can also get the amplitude of the hydrogen concentration variation around the mean value, and it is possible to infer whether these areas are rigid or not (i.e., how the nodes belonging to the same area behaves with respect to the adjacent ones.

[3] Once the surrogate model is trained, it can be used to replace the physical one to quickly perform variational analysis (e.g. Monte Carlo analysis) over a defined domain of input parameter variation or it can be used to simulate a series of varying inputs (e.g., a time series) to perform fast point-wise calculations.

The research leading to these results has received funding from Horizon 2020, the European Union's Framework Programme for Research and Innovation (H2020) under grant agreement n° 101111888.

The areas are the following:

1) Blue area: 0%$_{mol}$ hydrogen (on average):
   The nodes of this area exhibit a hydrogen concentration of 0 %$_{mol}$ over all the domain of variation. The fact that these same nodes have an associated standard deviation exactly equal to zero (that is the standard deviation of the inlet node #241, which does not exhibit variation), means that this portion of the network behaves exactly like the source node #241 from the point of view of the hydrogen concentration.

2) Dark red area: 10%$_{mol}$ hydrogen (on average)
   The nodes of this area exhibit an average hydrogen concentration of 10 %$_{mol}$ over all the domain of variation, with a standard deviation of 5.5 %$_{mol}$, which is the same of the inlet node #240 where blend of hydrogen is injected. Similarly to point one, this whole set of nodes behaves exactly like the source node #240.

3) Green area: ~ 5% hydrogen (on average)
   This is the area where the mixing always takes place resulting in a concentration of $[5.2 \pm 3.2]$ $\%_{mol}$.

4) Transitional "orange" area (highlighted by a black box in Figure 5-7):
   Unlike the previous areas, this small group of nodes displays a more heterogeneous behavior: the individual nodal average concentration varies in the range $[9.8 \div 8.0]$ $\%_{mol}$ with standard deviations in the range of $[5.5 \div 5.8]$ $\%_{mol}$, respectively. This implies that these nodes represent the moving boundary between the "blue area" and the "red area". It is to be noted that the average concentration value increases moving along the pipelines from the "blue area" to the "red area" showing that when the nearest node to the "red area" will still be most affected by the source with hydrogen blends.

A visualization of the network partition according to the average behaviour of nodal hydrogen concentration is given by the distribution diagram in Figure 5-7. For graphical reasons it would be difficult to indicate all the node ID labels in the network shown in Figure 5-6. However, the nodes labelled in the x-axis can be located in the specific zones on the network map following the same colour code.

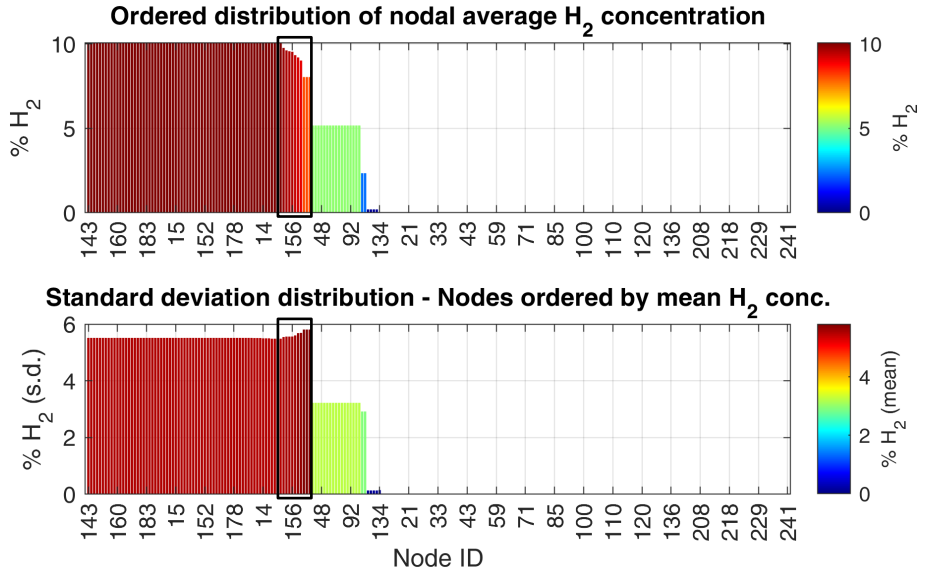

Figure 5-7: Distribution of the average nodal concentration and corresponding distribution of the standard deviation on the average value.

The research leading to these results has received funding from Horizon 2020, the European Union's Framework Programme for Research and Innovation (H2020) under grant agreement n° 101111888.

The information scattered throughout the network topology is here ordered to ease the partition and to show exactly each node's behaviour. The nodes have been ordered following a descending order of the hydrogen concentration. Correspondingly, the standard deviations are displayed following the same Node_ID order obtained with the above graph. Figure 5-7 supports, with quantitative features, the conclusions from the network graphs on Figure 5-6, which is useful to visualize the areas and to relate on a locational level the nodes. It should be noticed that Figure 5-7 highlights the presence of a couple of nodes (light blue bars on the mean value graph), which could not be observed for graphical reasons on Figure 5-6. These are located at the boundary with the "blue area", as better shown in Figure 5-8.

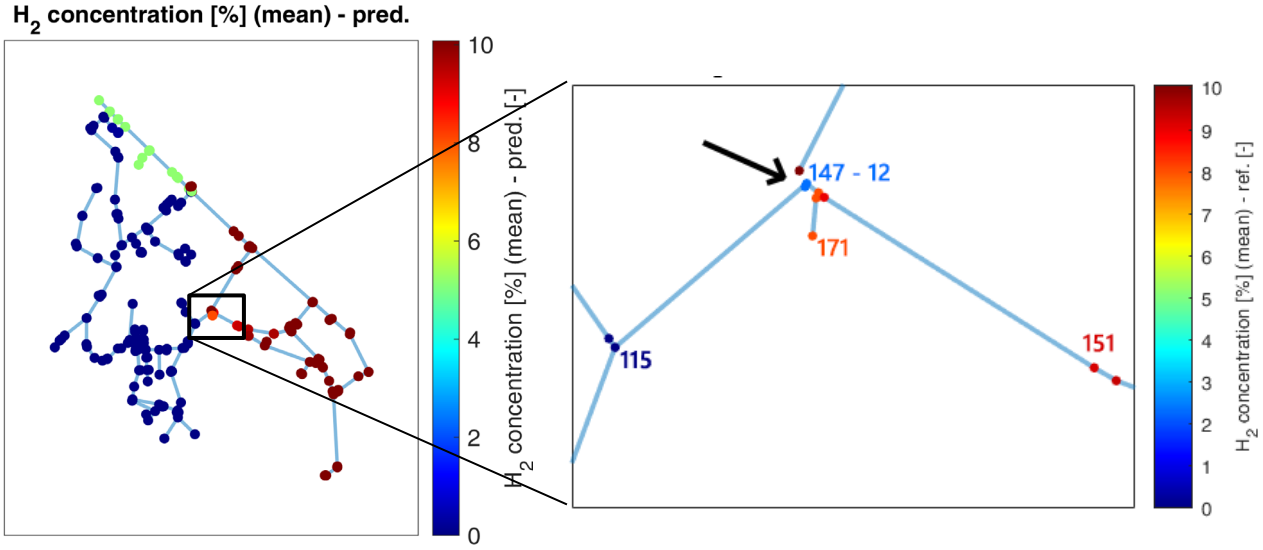

Figure 5-8: detail of the network infrastructure where the blue and the red areas borders.

It should be underlined that this analysis is carried out on average values over a wide domain of variation of 4 parameters. Focussing on the areas where the average hydrogen concentration deviates from the ones of the source node, it should be made the following distinction:

- Green area: this is a portion of the network where mixing always takes place. The resulting hydrogen share depends on the hydrogen concentration at the sources and the fluid-dynamics of the network.
- Orange transitional area: it defines a set of nodes which are, in turn, the boundary nodes between two adjacent gas composition areas. This mean that these nodes will not display a rigid behaviour form the point of view of mixing. Instead, depending on the fluid-dynamic condition of the network, some of them may take one of these different "states":

    - Same concentration of source 240
    - Same concentration of source 241
    - Mixed concentration → the node is the boundary between the two adjacent concentration areas.

  Thus this "transitional area" represents the area of the network where the boundaries of the concentration areas are moving, depending on the overall fluid-dynamics of the network.

The research leading to these results has received funding from Horizon 2020, the European Union's Framework Programme for Research and Innovation (H2020) under grant agreement n° 101111888.

5.2.1.2 Frequency analysis

A punctual (node-by-node) analysis can be done by analysing the distribution of the probability that a certain node displays a certain concentration with respect to one of the sources. In this case, it is relevant to consider the source where hydrogen is present.

The surrogate model for the concentration has been used to create a dataset of 1000 nodal concentration vectors, resulting from 1000 combinations of the 4 input parameters. Based on this dataset, the probability density function can be obtained for all the nodes. In the following (Figure 5-9, Figure 5-10) a selection for some representative nodes is given. Nodes: 115, 147, 171 and 151 are contiguous nodes located in the surrounding on the transitional area (see Figure 5-8). Node 75 is instead representative of the green area (Figure 5-10). In the figures, their probability density function has been superimposed to the one of the hydrogen blending source node (node 240).

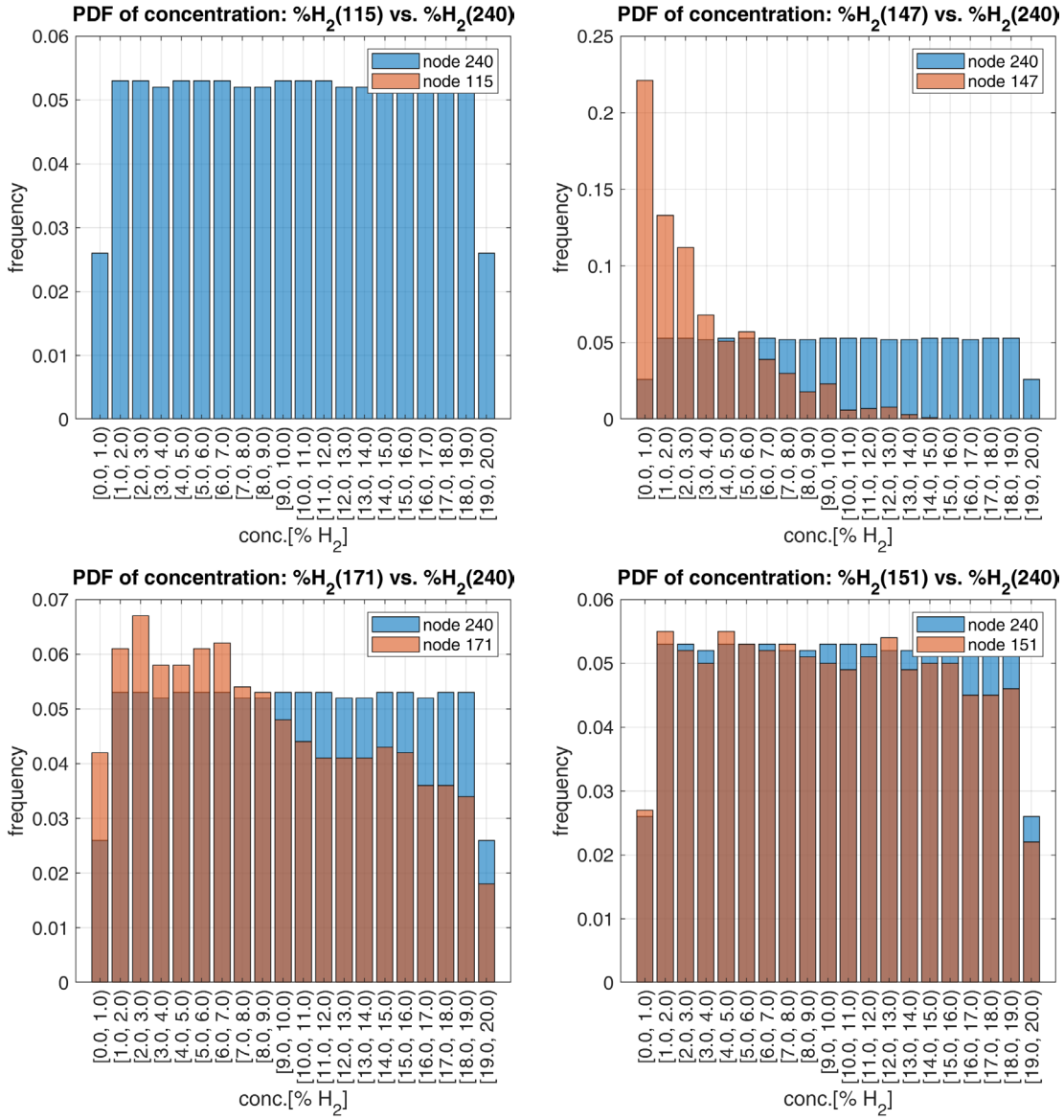

Figure 5-9: Probability density functions (PDFs) of the H_2 concentration of selected nodes of the "red" and "blue" quality area border, superimposed to the PDF of the blending source node 240.

The frequency is here sampled in 1% wide bins, from 0 to 20%$_{mol}$, and it has been evaluated over a MC simulation of 1000 samples originated from the uniform variation of 4 input parameters, among which the hydrogen concentration at the source node (240). Hence, it is to be reminded that this value is variable (this is the reason why the PDFs have been compared with the one of the source node). When one node displays a PDF exactly coincident with the one of node 240, then it means that this node behaves exactly as the source node 240 (i.e. it belongs to the red area).

Conversely, the graph of node 115 shows that its PDF is always equal to zero. This is the representative case for any node belonging to the blue area, which always behaves like the other source node (no hydrogen blending source).

Node 147 instead is representative of a node in which mixing takes place. This is in line with its location, at the boundary between the blue and the red area. The shape of the pdf testifies that it is more probable that the concentration is low or very low, thus mixing is more influenced by the non-blending source (node 241) rather than the other.

Nodes 171 and 151 are also mixing nodes, each characterized by their own PDF shape. Comparing the two distributions, keeping in mind their location on the network (see Figure 5-8) it can be noted that the further away we move from node 115 and 147, the less likely it is that this node is a mixing one: in fact the PDFs form 147 to 171 and 151 change their shapes towards adapting to the one of node 240.

Figure 5-10 depicts the frequency of the hydrogen concentration in node 75 that is representative of the nodes in the green area. the shapes clearly indicate a strong sensitivity to the non-hydrogen source, with the more likely mixes around 3 – 4 %$_{mol}$. Interestingly, no matter how high is the hydrogen concentration in 240, in node 75 (and all the green area) the hydrogen concentration will never exceed 17%$_{mol}$.

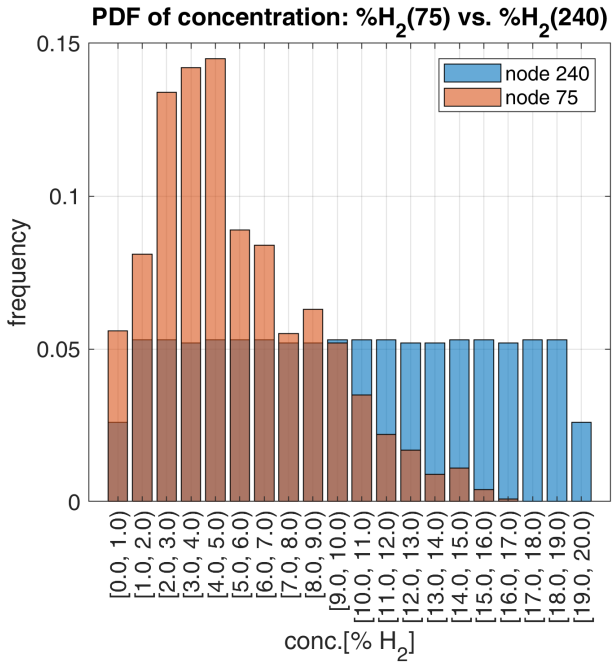

Figure 5-10: Probability density functions (PDFs) of the H_2concentration of a representative node of the "green mixing area", superimposed to the PDF of the blending source node 240.

The research leading to these results has received funding from Horizon 2020, the European Union's Framework Programme for Research and Innovation (H2020) under grant agreement n° 101111888.

The comparative analysis of the PDFs gives more quantitative information about the behaviour of each network nodes, especially with respect to the entry nodes. However, for the case of mixing nodes, especially on the transitional areas, it is not possible to verify whether they are always mixing nodes or, under some circumstances, they may display the same behaviour of one of the sources.

For this reason, the graphs in Figure 5-11 are given, for the transitional nodes 147, 171, 151

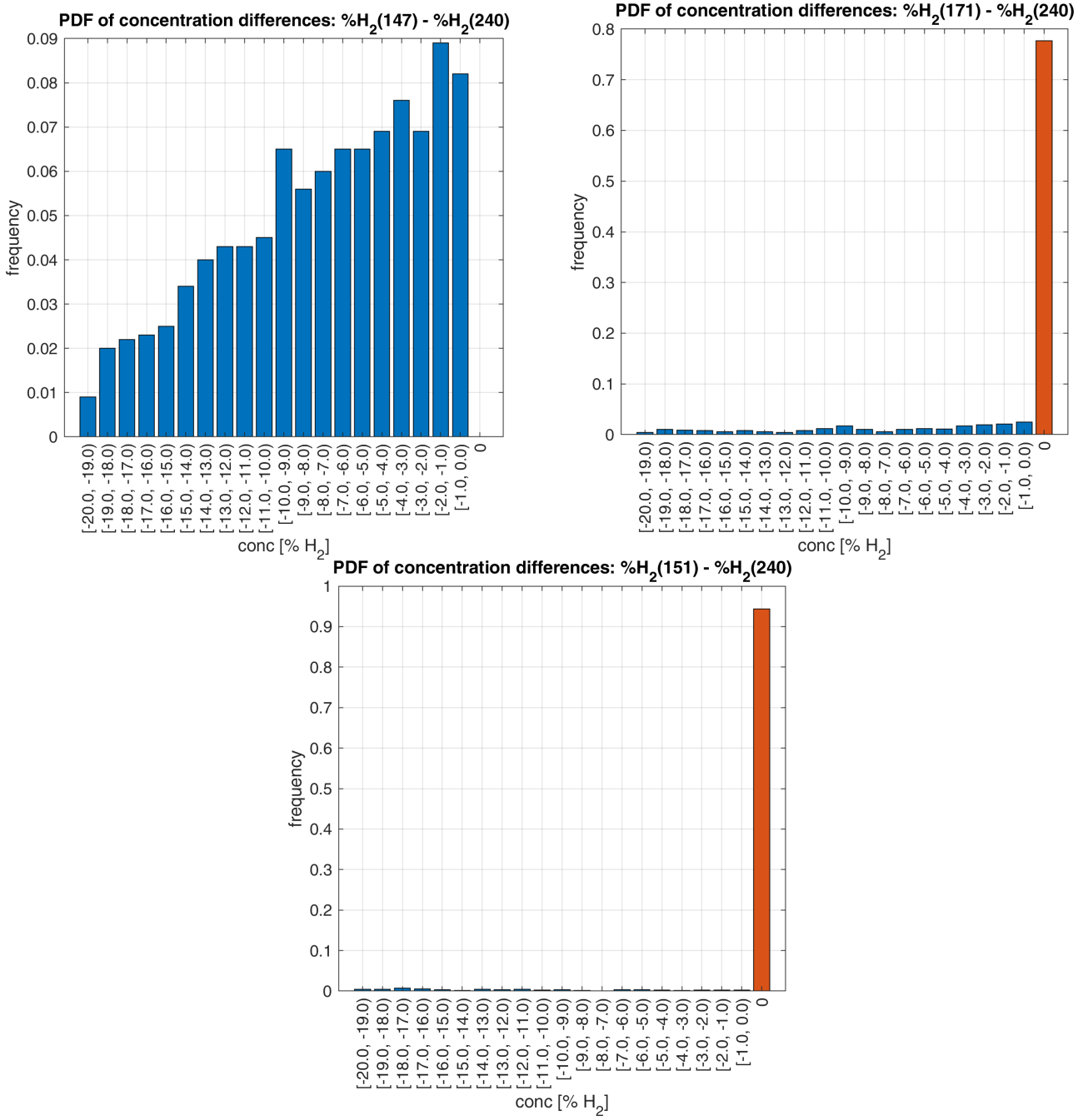

Figure 5-11: Probability density functions (PDFs) of the H_2concentration difference between selected nodes and the blending source node 240. The selected nodes belong to the "red" and "blue" quality area border.

Here the frequency distribution of the difference between the hydrogen concentrations at the specific node and the concentration of the source node is distributed in 1% wide bins, from 0 to – 20%$_{mol}$, plus one bin counting the occurrences when the difference is strictly equal to zero (the one highlighted in orange). In this way, it is possible to evaluate the probability that the specific node is not undergoing mixing but rather behaving as the reference source node.

So it can be inferred that node 147 is always a mixing node, while moving rightwards (with reference to Figure 5-8), the transition nodes 171 and 151, which displayed a different PDF than the source node, are still very likely to behave exactly like it (node 240). Here in fact, it is shown that for almost 80% of the times and more than 90% for respectively nodes 171 and 151, the behaviour is the same as the source node.

5.2.1.3 Global Sensitivity Analysis

The global sensitivity analysis is here discussed following the methodology presented in 4.2.3.1. The outputs on which this analysis is applied are the nodal concentrations of the previously selected nodes: 147, 171, 151. The aim is to evaluate which of the input parameters:

- $P \rightarrow$ nodal pressure set points
- $E \rightarrow$ pipeline roughness
- $G_{ext} \rightarrow$ nodal mass flow exchanged with the external environment (consumptions)
- $Y_1 \rightarrow$ hydrogen concentration in the blend set to enter from one of the two gas entry points.

has the highest impact on the variability of the nodal concentration of the selected nodes. The result is given in Figure 5-12.

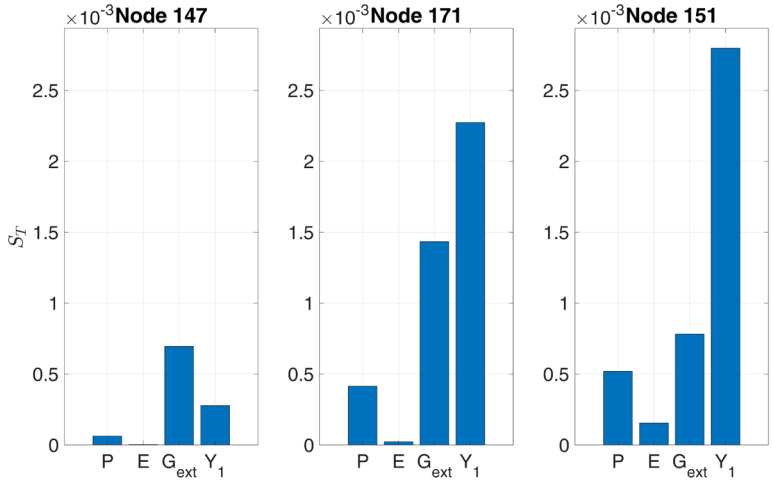

Figure 5-12: total-effect Sobol' indices for the concentration on the three selected nodes (147, 171, and 151) highlighting the individual contribution of the inlet pressure (P), pipe roughness (E), and consumption (G_{ext}) and blending source hydrogen concentration (Y_1).

It is worth noting that for node 147 the main contributor to the variability of hydrogen concentration is the consumptions G_{ext}, followed by the hydrogen concentration at the blending source Y_1. Node 147 is the node where mixing always takes place. In nodes 171 e 151, instead, the hydrogen concentration at the blending source Y_1 is the parameter having the most influence, followed by the consumption G_{ext}. It is to be reminded

The research leading to these results has received funding from Horizon 2020, the European Union's Framework Programme for Research and Innovation (H2020) under grant agreement n° 101111888.

that both nodes show a high likelihood to behave exactly like the source node (see comments to Figure 5-11) with residual frequency to be mixing nodes. Also, nodes 151 is closer to the red area – the one in which nodes are always behaving like the blending source one. Thus, the influence of the parameter Y_1 on the nodal concentration seems to increase as one moves towards the red area. In fact, this is proved by the Sobol' analysis on two nodes within the red area: node 240 (the blending source node) and node 178, randomly chosen within the area. The results are displayed in **Figure 5-13**.

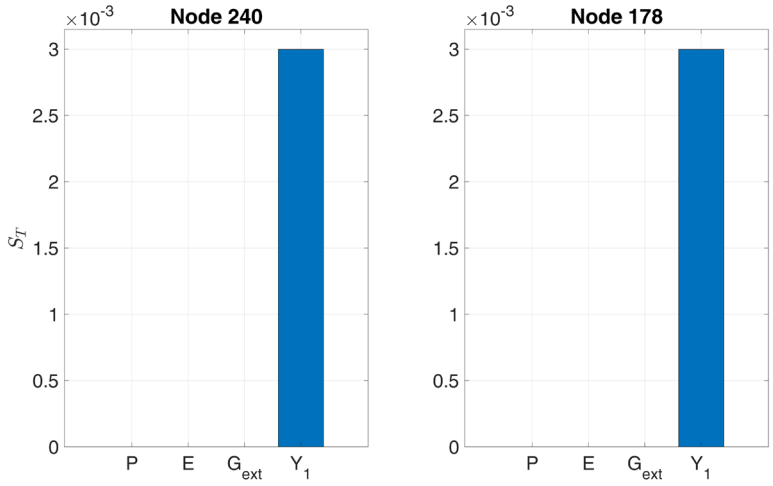

Figure 5-13: total-effect Sobol' indices for the concentration on two selected nodes belonging to the red area (240, 178) highlighting the individual contribution of the inlet pressure (P), pipe roughness (E), and consumption (G_{ext}) and blending source hydrogen concentration (Y_1).

The only parameter influencing the nodal concentration is parameter Y_1. Node 178 is influenced in the very same way as the blending source 240. Under the point of view of the nodal concentration, the whole red area is affected just by parameter Y_1, proving that all the nodes belonging to the area behaves as the blending source node. Calculating the total effect Sobol' indices for the concentration of the nodes of the blue area would return zero for all the parameters. In fact, there is no variation of concentration in the area and the concentration value is always zero.

For the sake of completeness, in Figure 5-14 the results of the Sobol' indices analysis on three randomly chosen nodes belonging to the green area are displayed. For this mixing area, the result is that the blending source concentration is the most impactful parameter, followed by the consumption. This might be due to the location of this area in the network: it is a peripheral area where contributions from both gas sources converge. However, it is not interested much by significant changes in pipeline gas flows (e.g. gas flow direction): the further mixing happens in one node and further spread downstream, no matter what is the consumption level.

The research leading to these results has received funding from Horizon 2020, the European Union's Framework Programme for Research and Innovation (H2020) under grant agreement n° 101111888.

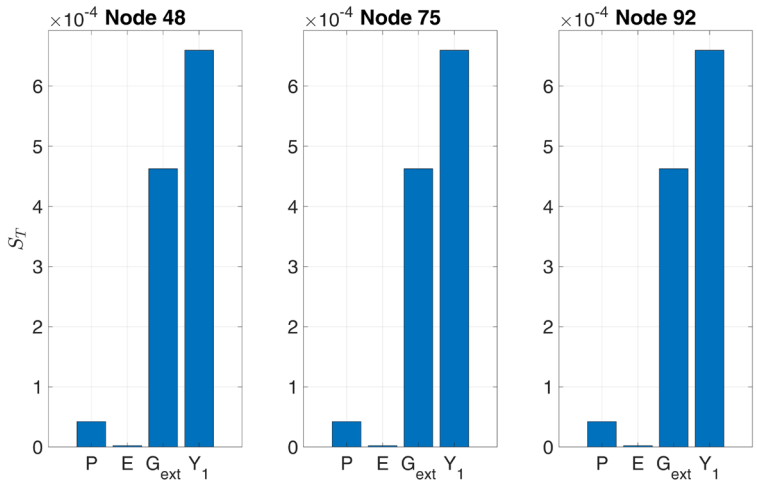

Figure 5-14: total-effect Sobol' indices for the concentration on three selected nodes belonging to the green area (48, 75,92) highlighting the individual contribution of the inlet pressure (P), pipe roughness (E), and consumption (G_{ext}) and blending source hydrogen concentration (Y_1).

5.2.1.4 Discussion

This test case describes a distribution network subjected to hydrogen blends incoming from one of the two gas entry points. The main fluid-dynamic set points (pressure set points at the gas entry points and gas consumptions at the customer/exit nodes) varies rigidly on a certain range representing a variety of operational points. Also, the technical parameter of the inner roughness of the pipelines (whose variation may represent scenario infrastructure aging pronounced) is varied, extending the domain. What is more, the hydrogen concentration at the inlet node is varied in the range $[0.5\%_{mol} \div 19.5\%_{mol}]$, allowing a very wide range of variation under the hydrogen composition point of view.

The surrogate model that has been generated is then able to reproduce very precisely the network response throughout all this wide range domain. The carried-out analysis focuses on the quality tracking and overall network impact of hydrogen blending and blending variations and it has been conducted over the whole domain covered by the surrogate model.

First the network-wide average nodal hydrogen concentration has been analysed, allowing to infer how the hydrogen blends propagate throughout the network under the many possible network operating and technical configurations. It is shown that the network behaviour is quite stable, with three well defined concentration areas which are formed. The boundaries of these concentration areas are the critical point of the network under a gas quality management point of view: it is observed that in these nodes, gas quality (in this case hydrogen concentration) may switch from the concentration of one source, or the other or even further mixing can happen.

In this specific case study, it was possible to spot a specific pipeline along which the boundary between the area with the higher hydrogen concentration and the area with no hydrogen "moves". Through a detailed analysis of the probability density function of hydrogen concentration at each of these "critical" nodes, it was possible to further investigate their individual behaviour. In fact, it was possible to distinguish among the nodes where gas mixing always takes place and the ones which switch from the same concentration as all the nodes of their area and intermediate mixing. More specifically, it was observed that the probability for these nodes to display mixing was very low (< 80 – 90 %) thus implying that anyways the localization of the boundaries

The research leading to these results has received funding from Horizon 2020, the European Union's Framework Programme for Research and Innovation (H2020) under grant agreement n° 101111888.

between the quality areas is quite steady. What is more, the further the node is from the fully mixing nodes, the less likely it is for it to have mixing, adhering to the behaviour of all the other nodes of the area. This analysis allows also to check the distribution of the concentration of the mixing node across the hydrogen blending variation inferred by the variation of the source. In this regards, for example, it is interesting to comment on the average behaviour of the "green area" of the network (ref. Figure 5-6 and Figure 5-10): here a lower hydrogen blends is (almost) always formed: on average the hydrogen concentration is about $5.2\%_{mol}$ with a standard deviation that is $3.2\%_{mol}$: in absolute terms a further blending leads to smaller variations on the average values, narrowing the width of possible hydrogen concentrations. However, in relative terms the hydrogen concentration variability is more pronounced.

All these outputs and consideration are obtained from the use of the surrogate model and are useful tools to interpret the network behaviour with local hydrogen blending and its variability. For example, defining the network areas characterized by homogeneity of hydrogen concentration, localizing the nodes which can possibly be the boundaries of these areas and quantifying the probability (or frequency) of mixing or non-mixing in these nodes can help to manage the gas quality control of the network. After this kind of analysis, the location of gas quality monitoring system can be performed and also the definition of maximum range of variability in hydrogen concentrations can be defined, in view of gas quality transparency towards final users. Also, knowing how the gas quality changes and how the network can be divided into sub-areas of homogeneous quality contribute to a fair allocation of heating values for billing purposes.

To be highlighted that all the network states which have been used to draw a synthesis represent steady state (hence equilibrium state) of the network.

5.2.2 5 input parameters with two hydrogen injections

This scenario represents the extension of the previous one to cases in which both the gas entry points are characterized by some hydrogen blending. Thus, one input parameter has been added that is the hydrogen concentration at the second gas inlet point (node 241). The variability of hydrogen blending at node 241 has been assumed to be the same as node 240: both nodes undergo a hydrogen composition variation in the range $[0.5\%_{mol} \div 19.5\%_{mol}]$. Given that the hydrogen concentration at the two sources varies independently, the surrogate model is trained over a wide domain, encompassing wide blending variability for both the sources. This allow the surrogate model to be used for any combination of hydrogen blending level from each individual source, choosing independently a variation rage, as long as it is included in the overall domain of variation investigated in this application case. An example is given in the following paragraph where the model is applied to a subdomain in which the blending set points and the relative variation are differentiated.

In the next first portion of this paragraph, only a brief analysis will be presented, as what has been obtained and presented in 5.2.1.1 can also be repeated with this more general surrogate model, resulting in different results but, on a methodological level, the same observations and discussions.

5.2.2.1 Concentration distribution

Analyzing the average concentration distribution obtained with the surrogate model used for a MC simulation using 1000 trials with uniform distribution over the whole domain of variations lead to the graphs in Figure 5-15

The research leading to these results has received funding from Horizon 2020, the European Union's Framework Programme for Research and Innovation (H2020) under grant agreement n° 101111888.

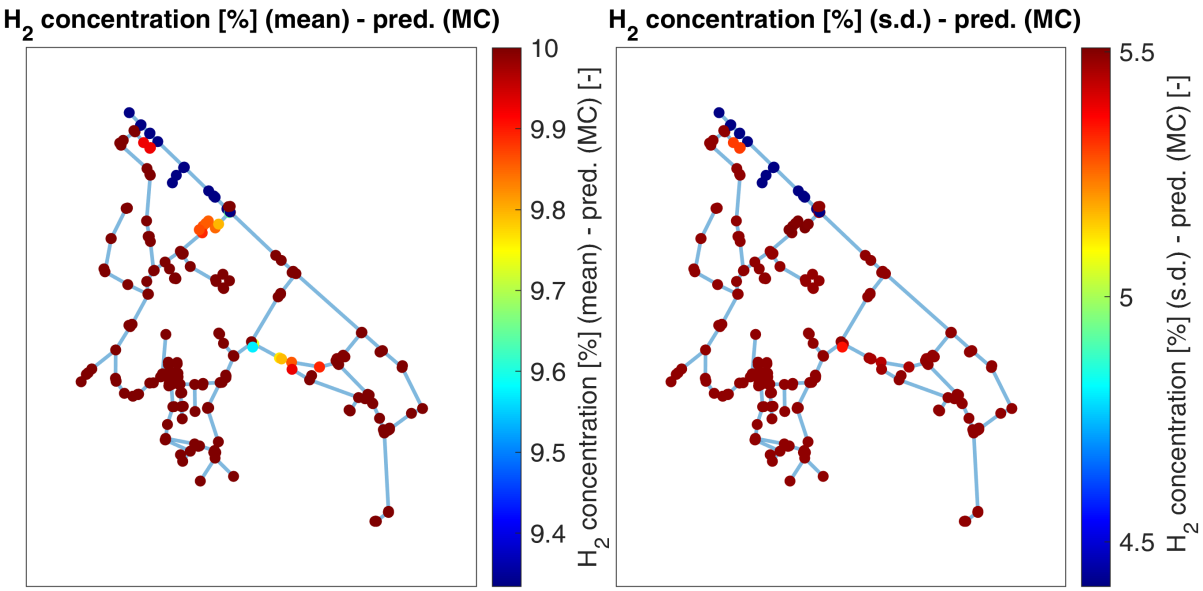

Figure 5-15: left: nodal hydrogen concentration as obtained from the surrogate model run with a Monte Carlo simulations of 1000 trials. The concentration values are averaged over the whole parametric domain; right: related standard deviation.

On average terms, the hydrogen concentration throughout the network is more uniform than in the previous case as both the sources varies in the same way but independently. The graph on the left shows clearly a persistent mixing area (the blue one) and the boundary nodes between the different areas of the network. In this more general case, the "network areas" are portion of the network (i.e. group of nodes) which displays a behaviour exactly equal to one of the two source or equal to a mixing point which influences all the downstream nodes (this is the case of the "blue area" in Figure 5-15). The boundary nodes have a complex behaviour and show that in there mixing can happen and/or they can behave the same as the other nodes of the adjacent area, depending on the circumstances.

The main feature of this version of the surrogate model is that both the sources can be tested with different and variable hydrogen concentrations. Using the same surrogate model the following Monte Carlo analysis is carried out to show more clearly the potentialities of the tool and to better highlight the results which can be obtained.

Application of the surrogate model to a different subdomain: variation of the hydrogen blend around different set-points.

Let's now consider the sub-test with the following domain of variation:

- Par.1) Entry pressures at both ReMi stations (with a variation $\Delta P = \pm 7$ %);
- Par.2) **H2 blending at the primary ReMi station ($5\%_{mol} \pm \Delta H = \pm 10$ %);**
- Par.3) **H2 blending at the secondary ReMi station ($10\%_{mol} \pm \Delta H = \pm 50$ %)**
- Par.4) Pipeline roughness ($\Delta E = \pm 10$ %);
- Par.5) Exit flow to Riccione users ($\Delta G_{ext} = \pm 20$ %).

A MC simulation using 1000 trials with uniform distribution over the whole domain of variations is performed, leading to the following results (Figure 5-16):

The research leading to these results has received funding from Horizon 2020, the European Union's Framework Programme for Research and Innovation (H2020) under grant agreement n° 101111888.

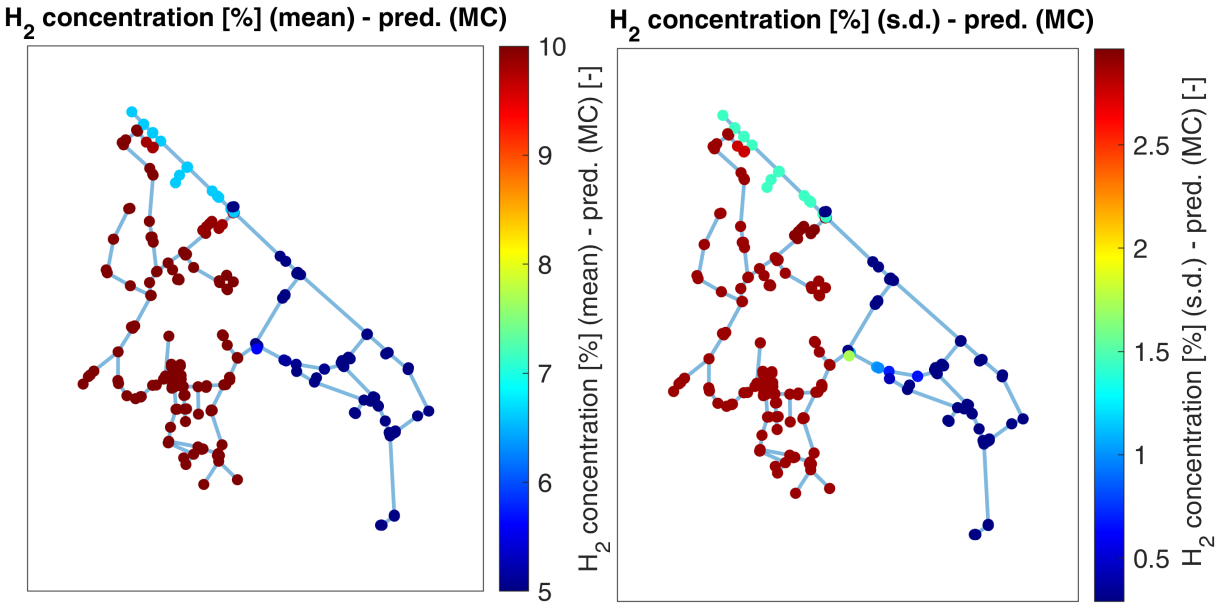

Figure 5-16: left: nodal hydrogen concentration as obtained from the surrogate model run with a Monte Carlo simulations of 1000 trials. The concentration values are averaged over the whole parametric domain; right: related standard deviation.

Figure 5-17 provides the corresponding nodal concentration distribution which ease the partition of the network in homogeneous quality areas. Besides the evident areas with constant hydrogen concentration (and equal to the respective source), it can be noted that there are a group of nodes which displays average hydrogen concentration slightly lower than 10%$_{mol}$ and some other which displays concentration slightly higher than 5%$_{mol}$.

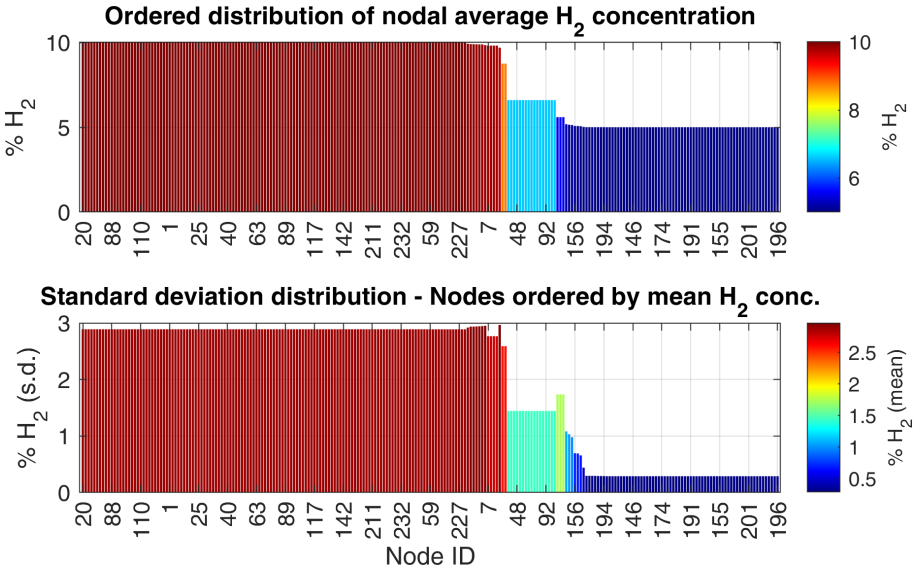

Figure 5-17: Distribution of the average nodal concentration and corresponding distribution of the standard deviation on the average value.

The research leading to these results has received funding from Horizon 2020, the European Union's Framework Programme for Research and Innovation (H2020) under grant agreement n° 101111888.

These nodes are highlighted in **Figure 5-18**. The location on the network map shows that these nodes are the ones belonging to the so-called moving boundaries of the different quality area of the network.

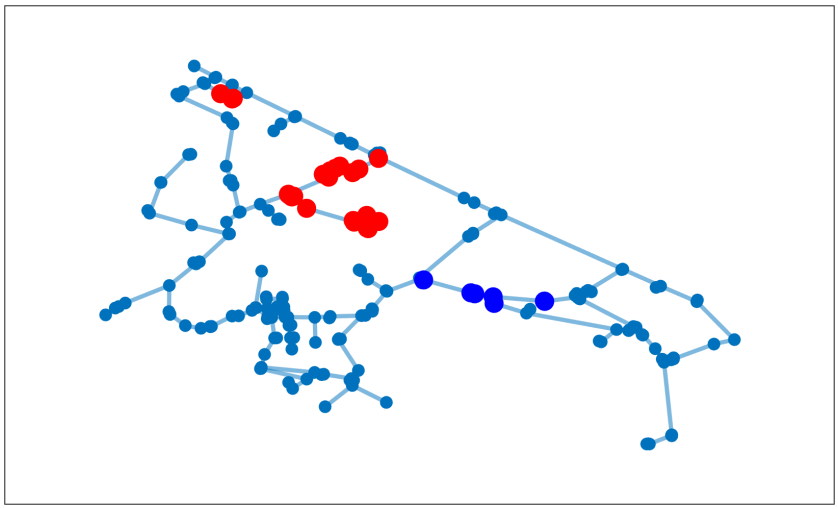

Figure 5-18: Gas network topology with the nodes belonging to the moving boundaries highlighted in red and blue.

These nodes have more complex behaviour with respect to the others, and their detailed analysis may be worthy, together with the analysis of the mixing nodes. On the other hand, the results in this specific case shows that the average hydrogen concentration in these nodes have a very small difference with respect to one of the adjacent area, thus the network operator can decide to allocate them to the same quality area, with the support of quantitative results.

Nodal frequency analysis and global sensitivity analysis are not presented for this case study for the sake of conciseness of this deliverable. Following the same rationale as the one of paragraph 5.2.1, the analysis can be carried on the nodes highlighted here, getting to similar but case specific conclusions.

5.2.2.2 Discussion

With this test case the parametric analysis by means of surrogate models has been extended to the case where both the gas inlets have a variability in the hydrogen gas quality. This case is relevant for those networks where more than one possible hydrogen injection point is foreseen. The independent variability of the hydrogen concentration at the inlets can simulate different operating conditions of the hydrogen production facilities, allowing the analysis of the impact on the network and the acceptability from the network side of multiple sources with concentration that are variable within a certain range.

5.2.3 30 input parameters with two hydrogen injections

A remarkable generalization is obtained here. The same infrastructure is here tested over a variation domain consisting of 30 dimensions. With respect to the previous cases, two main differences have been introduced:

- Pressure set points: two independent variables;
- Gas consumptions: localization of 25 consumption clusters with independent variation.

The introduction of these dimensions allows the case study to be representative of more complex operating conditions in which the distribution networks may be operated in reality. Specifically, having separated the

The research leading to these results has received funding from Horizon 2020, the European Union's Framework Programme for Research and Innovation (H2020) under grant agreement n° 101111888.

variation of the pressure set points means that the domain of variation can cover all the operating condition in which the roles of the gas entry points are switched: the one that usually is the primary entry station (the station operated at higher pressure set point) becomes secondary and vice versa. Moreover, the splitting of the gas consumption in clusters introduces the possibility to investigate the possibly complex and uncorrelated behavior of gas consumption throughout different users or (better) different areas of the network. In this specific infrastructure, the different gas consumption clusters represent the Final Reduction Stations (FRS i.e. the points of the network where the gas undergoes the last pressure reduction to mbar level through a throttling valve). Through FRSs, the gas is transferred to the portion of the infrastructure where individual final users are actually connected.

The independent variation of the gas consumption of each FRS represents variation in the geographical distribution of the consumption. However, it is to be underlined that in this specific case each variation is completely uncorrelated with respect to the others. On the one hand, it allows a very general, out-of-domain representation of the possible network operating conditions and configurations. On the other hand, it might be a too general representation: even though some relative variation among the gas exit flows at the FRS are common, the gas consumption of each final user of a distribution system tends to follow a common tendency on a daily, weekly and seasonal basis. So, in the most realistic scenario, the local variation of gas consumption should be seen as an additional (and independent) term of variation of a common variation in gas consumption.

The surrogate model that is addressed in this section covers instead the full range of variation of the gas consumption of the different clusters as if they were totally uncorrelated. Thus, in principle, the most realistic cases can be addressed with the same surrogate model, being a subset of the most general framework.

5.2.3.1 Concentration distribution

Figure 5-19 displays the topological distribution of the average concentration (left) and the corresponding standard deviation (right) obtained from a MC simulation with 1000 trial, using the surrogate model.

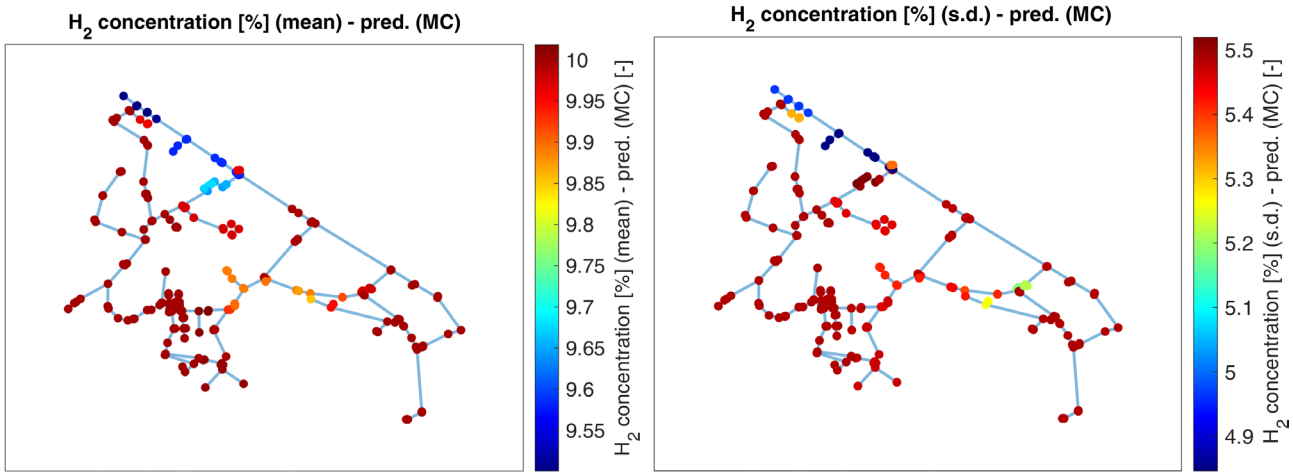

Figure 5-19: left: nodal hydrogen concentration as obtained from the surrogate model run with a Monte Carlo simulations of 1000 trials. The concentration values are averaged over the whole parametric domain; right: related standard deviation.

Similarly to what is observed in the previous case, on average terms the hydrogen concentration tends to the nominal value set at the entry nodes, around which the concentration input parameter varies. Again, the areas where the average concentration is slightly different highlights the presence of mixing among the two sources. These are the same nodes where the standard deviation differs the most than the one characterizing the source

The research leading to these results has received funding from Horizon 2020, the European Union's Framework Programme for Research and Innovation (H2020) under grant agreement n° 101111888.

nodes, testifying a different behavior. With respect to the case with 5 parameters, the nodes which deviates from the source behavior are more and more spread throughout the network, showing that having added parameter of variation have implied a more complex behavior of the network.

Following the same sequence of the previous sub-paragraph, the same surrogate model has been applied to a more specific case study in which the nominal concentration at the inlet nodes has been differentiated and so the respective variation.

Application of the surrogate model to a different subdomain: different variation of the hydrogen blend around different set-points.

Let's now consider the sub-test with the following domain of variation:

- Par.1) Entry pressures at primary ReMi stations (with a variation $\Delta P = \pm 7$ %);
- Par.2) Entry pressures at secondary ReMi stations (with a variation $\Delta P = \pm 7$ %);
- Par.3) **H2 blending at the primary ReMi station ($5\%_{mol} \pm \Delta H = \pm 10$ %);**
- Par.4) **H2 blending at the secondary ReMi station ($10\%_{mol} \pm \Delta H = \pm 50$ %)**
- Par.5) Pipeline roughness ($\Delta E = \pm 10$ %);
- Par.6-30) Exit flow to Riccione users ($\Delta G_{ext} = \pm 20$ %).

A MC simulation using 1000 trials with uniform distribution over the whole domain of variations is performed, leading to the following results (Figure 5-20):

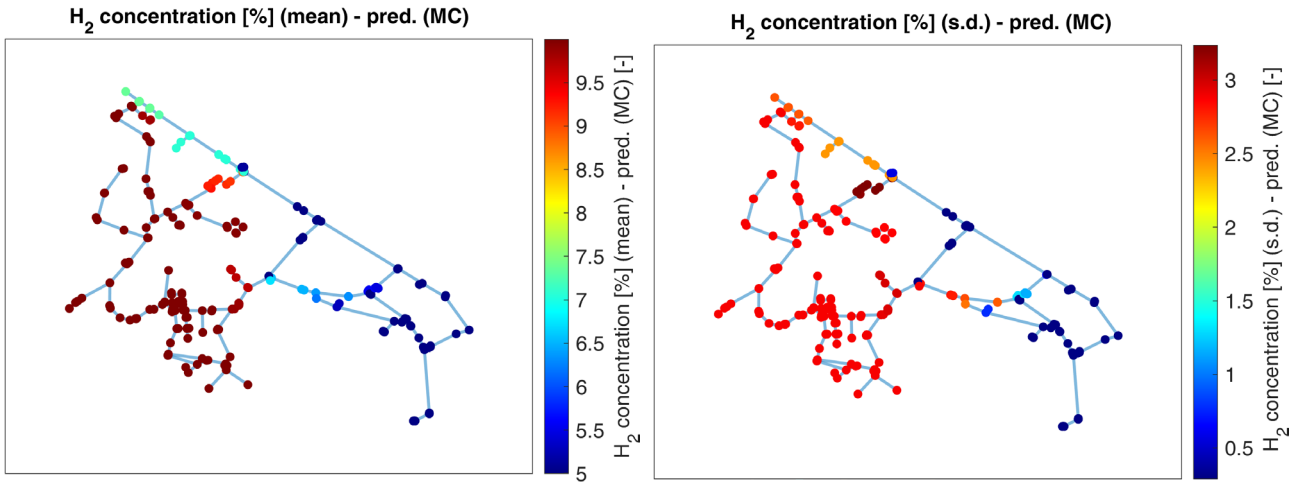

Figure 5-20: left: nodal hydrogen concentration as obtained from the surrogate model run with a Monte Carlo simulations of 1000 trials. The concentration values are averaged over the whole parametric domain; right: related standard deviation.

Figure 5-21 provides the corresponding nodal concentration distribution. Unlike the previous cases, the transition to the most frequent concentration levels is more gradual, thus the clear definition of areas with homogeneous quality is harder. This is expected because the gas consumptions and the two pressure set points at the network inlets varies in an uncorrelated way throughout the network. However, the effect of this variability on the gas composition is still limited to certain number of specific nodes which are localized by means of this methodology. What is more, the graph on the standard deviation gives information on the width of variation, allowing a good definition of the behaviour of these nodes. Wide areas with constant hydrogen concentration (equal to the respective source) are still well defined.

The research leading to these results has received funding from Horizon 2020, the European Union's Framework Programme for Research and Innovation (H2020) under grant agreement n° 101111888.

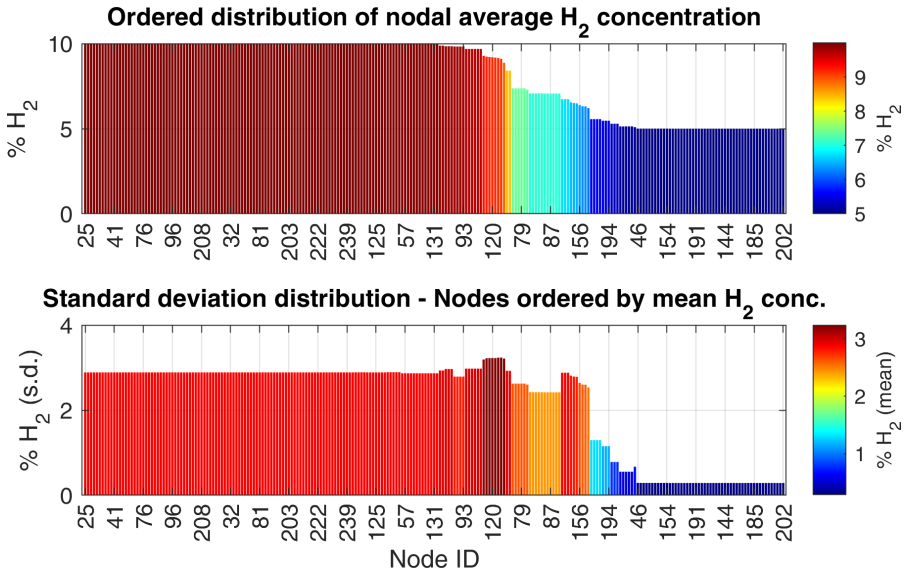

Figure 5-21: Distribution of the average nodal concentration and corresponding distribution of the standard deviation on the average value.

5.2.3.2 Global Sensitivity Analysis

A few nodes have been selected for the global sensitivity analysis. These nodes have been chosen to be representative of the areas of the network where the average behavior is different than the source nodes. In Figure 5-22 the map of the network with the position of the chosen node highlighted is given. Besides, also the FRSs nodes (representing the consumption clusters) have been pinpointed.

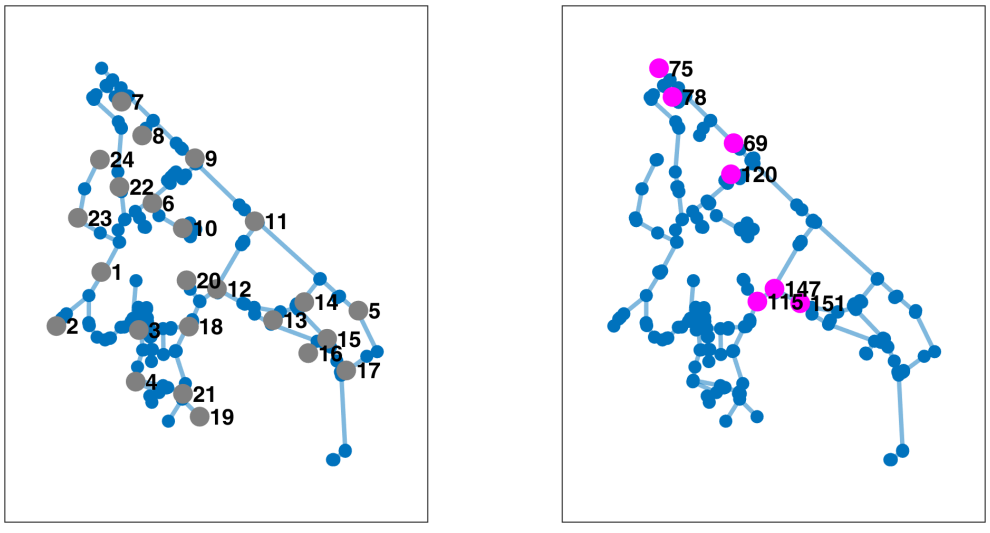

Figure 5-22: Gas network topology with the gas consumption cluster nodes highlighted in grey (left) and the investigated nodes highlighted in pink (right).

The research leading to these results has received funding from Horizon 2020, the European Union's Framework Programme for Research and Innovation (H2020) under grant agreement n° 101111888.

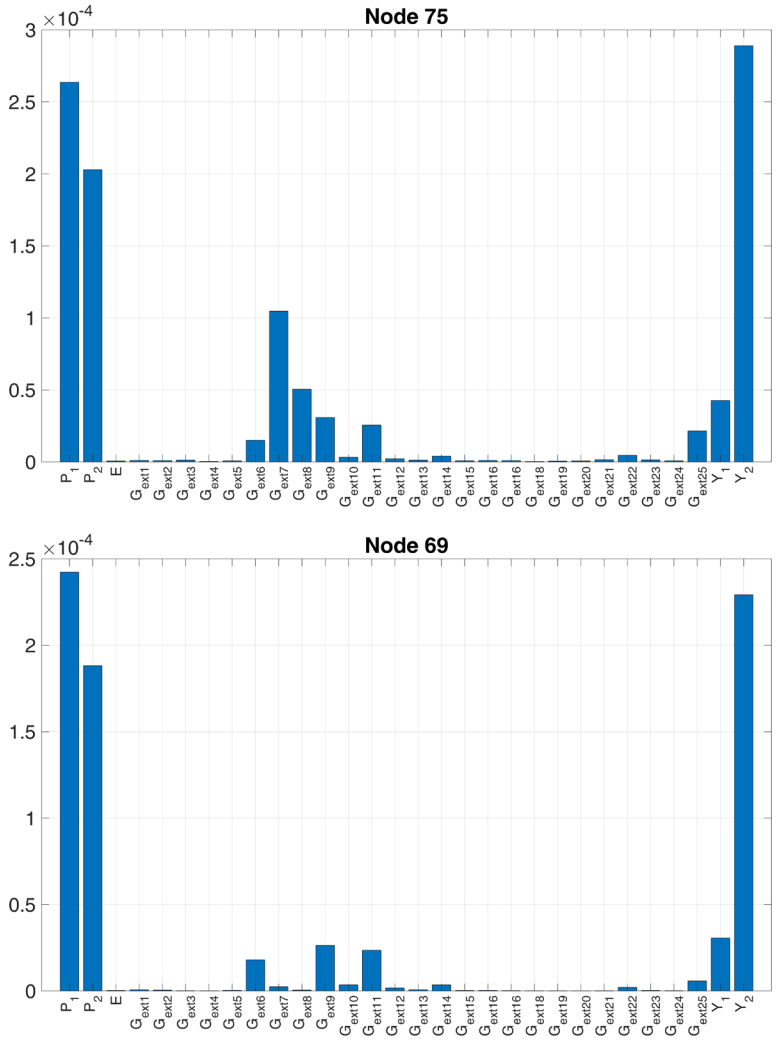

Figure 5-23: total-effect Sobol' indices for the concentration on the nodes 75 and 69 (north-east mixing area of the network). It highlights the individual contribution of the inlet pressure set points (P_1 and P_2), pipe roughness (E), the different consumption clusters ($G_{ext1} – G_{ext25}$) and blending sources' hydrogen concentration (Y_1 and Y_2).

Figure 5-23 shows the global sensitivity analysis on the hydrogen concentration of two nodes belonging to the main mixing area – the north-east portion of the infrastructure. Unlike previous test cases, the behaviour of in this area is more complex and, from the analysis of the average concentration, it is possible to define two sub-areas, even though they differ by less than 1% of hydrogen. Node 75 is representative of the nodes displaying the higher concentration. Form the comparison of the two graphs in Figure 5-23, it is clear that the concentration in these two nodes is more sensible to different parameters. While for both nodes the main influencing parameters Y2, P1 and P2, node 75 displays clearly that Y2 is predominant over the pressures while in node 69, the role of P1 seems to be slightly higher. To be reminded that Y2 is refers to the concentration variation at the second inlet node (node 241) which is nearer to these nodes. Also, the role of both pressure set points is significant for both nodes, with P1 always higher than P2. This relation between the two might be due to the fact that the nominal value of P1 has been kept higher than the one of P2, even though the range of variation is such that sometimes (but less frequently) the set point P2 can be higher than P1, contributing to the complexity of the case. Focussing on the relative contribution of the individual gas

The research leading to these results has received funding from Horizon 2020, the European Union's Framework Programme for Research and Innovation (H2020) under grant agreement n° 101111888.

consumption variation of the cluster nodes it can be noted that in both cases, the greater impact is given by the nodes which are close to the investigated one in terms of network topology.

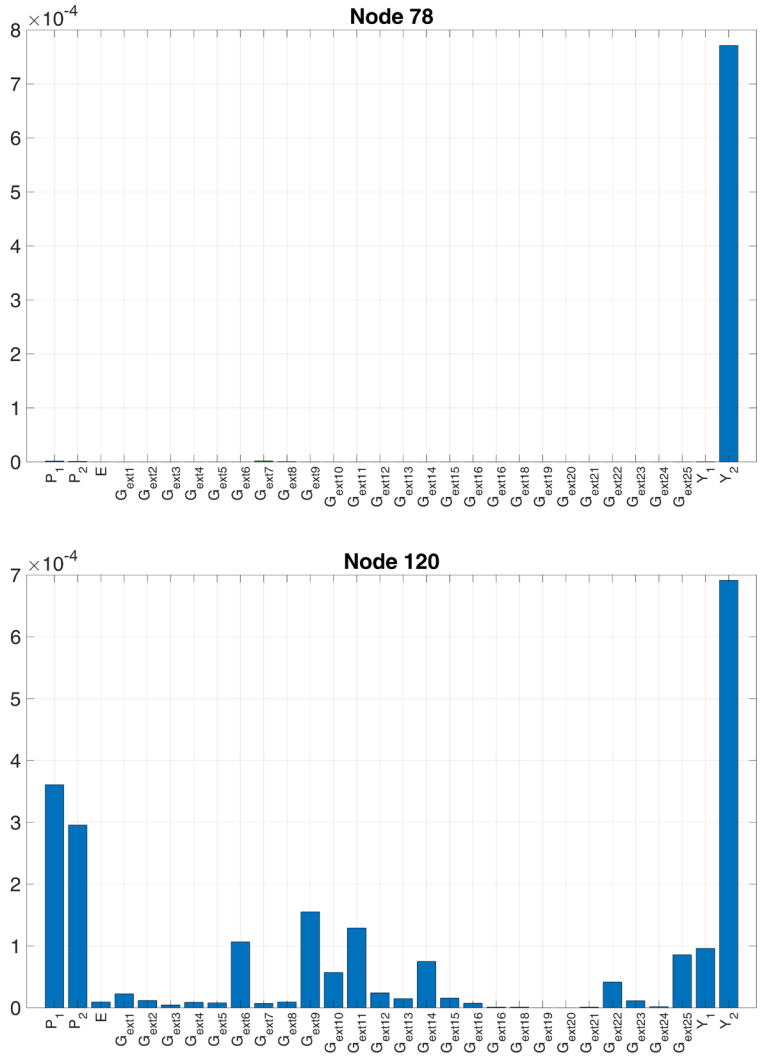

Figure 5-24: total-effect Sobol' indices for the concentration on the nodes 78 and 120 (boundaries with north-east mixing area of the network). It highlights the individual contribution of the inlet pressure set points (P_1 and P_2), pipe roughness (E), the different consumption clusters ($G_{ext1} - G_{ext25}$) and blending sources' hydrogen concentration (Y_1 and Y_2).

Figure 5-24 addresses two nodes belonging to the boundaries of the north east mixing area with the adjacent areas. The difference in these global sensitivity analysis is noteworthy: the concentration in node 78 is influenced by the concentration in Y2 only (it is to be noted that on average terms its concentration is very near to the one of the second inlet node where Y2 is set, in fact). Concentration in node 120 shows a more varied sensibility throughout all the parameters (which matches to the fact that on average terms the concentration differs more than the one of source 2, which anyways is the most influential parameter. As for nodes 75-69, pressures are the following most influential parameters. The relative contribution of the different consumption clusters reminds the one of node 69 even though some difference can be noted: first, the contribution of the gas consumption variation in the most relevant clusters is closer to the contribution of the pressure parameters. Then, how each cluster influences the concentration in node 120 is similar to what

The research leading to these results has received funding from Horizon 2020, the European Union's Framework Programme for Research and Innovation (H2020) under grant agreement n° 101111888.

observed for node 69 but with some peculiarities: indeed, the two nodes are close to each other, still their position on the network influence the role of each consumption cluster (e,g, see the role of G_{ext14} in N120 and in N69.).

Figure 5-25 displays the global sensitivity analysis on the concentration of three nodes belonging to the boundary between the two areas always influenced by the concentration of one of the two entry points. This boundary was already highlighted in the previous, simpler test cases. In this one, because of the increased number of independently varying parameters, the localization of this boundary is less straightforward. The average concentration analysis in Figure 5-20 shows a faded behavior, in fact. Nodes 115, 147, and 151 are localized along this transitional region.

The concentration in node 115 is clearly dominated by the behavior of the concentration sets in the inlet node 241, with a residual role given by the pressure set points. The role of the pressure set points is increased in the sensitivity analysis on the concentration of node 147, even though it is still dominated by the parameter Y2 as for node 115. Interestingly, node 151 displays instead a different behavior: the pressure set points are the parameter which influence the most the concentration, followed by the concentration in node 241 (Y2). Then comes Y1, which shows a comparable impact as the one of a few consumption clusters. The most influential consumption clusters are different from the ones highlighted in the previous comments. The consumption clusters which impact the most the concentration in node 151 are the closer to the addressed node.

The research leading to these results has received funding from Horizon 2020, the European Union's Framework Programme for Research and Innovation (H2020) under grant agreement n° 101111888.

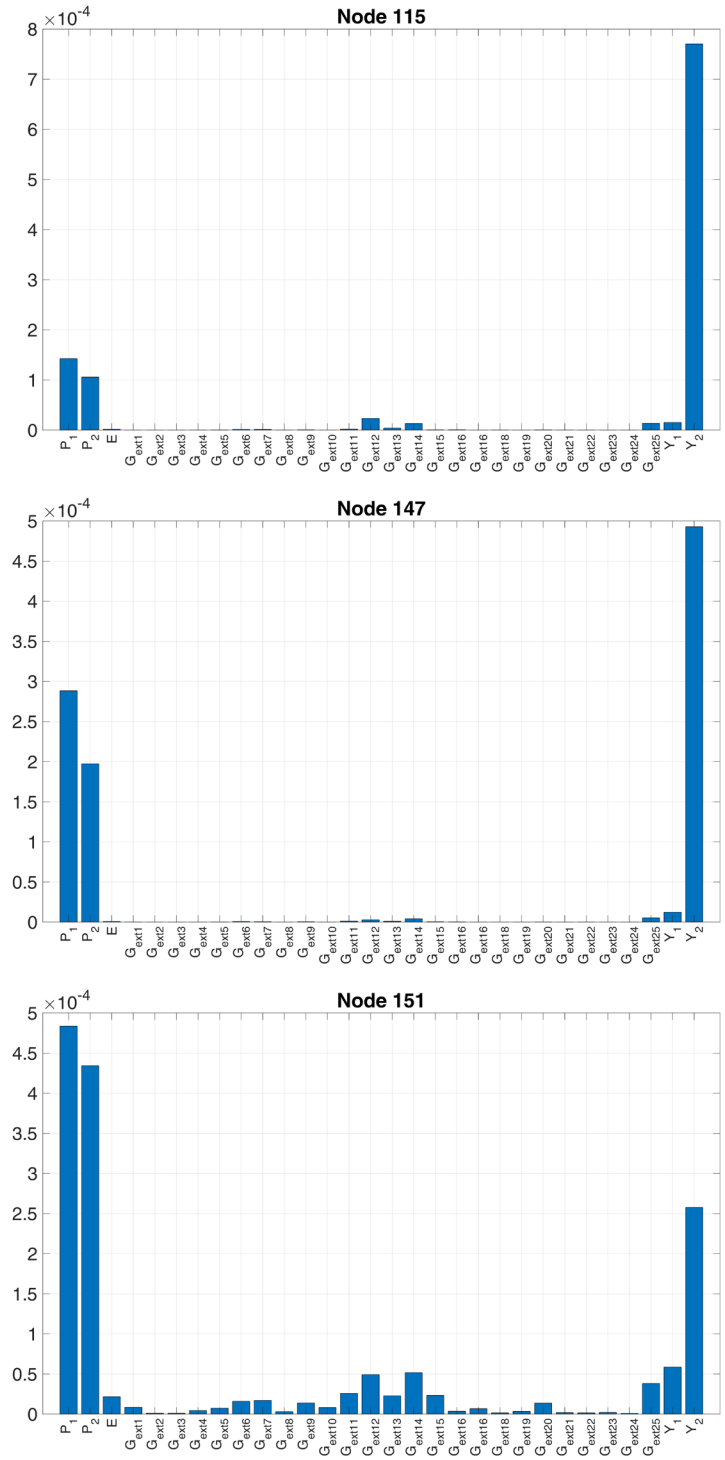

Figure 5-25: total-effect Sobol' indices for the concentration on the nodes 115, 147, and 151 (boundary between the blue and the red area). It highlights the individual contribution of the inlet pressure set points (P_1 and P_2), pipe roughness (E), the different consumption clusters (G_{ext1} – G_{ext25}) and blending sources' hydrogen concentration (Y_1 and Y_2).

The research leading to these results has received funding from Horizon 2020, the European Union's Framework Programme for Research and Innovation (H2020) under grant agreement n° 101111888.

5.2.3.3 Discussion

With respect to the two previous case, the distribution network is subjected to a much higher dimension domain of variation having set completely independent variation on the main fluid-dynamic set points: the two pressure set-points and the main gas consumption cluster – which are represented by 24 final reduction station + 1 cluster which includes all the final users directly connected to this tier of the infrastructure.

The possibility to take into account scenarios with a different geographical distribution allows, in this specific model of this specific distribution infrastructure, to simulate scenarios in which the final reduction stations (FSR) are regulated in a different manner than the nominal set point, thus inferring a change in the hierarchy with which they are feeding the downstream network. Through a modification of the outlet pressure set point of the FSRs, the gas flux exiting the higher-pressure level and feeding the lower pressure level through the station changes. From the perspective of the higher-pressure level network, a change of the exiting gas flow rate is seen. This is exactly what this 30-parameter test case can represent.

This complex and variable domain allows a more realistic model of the gas infrastructure, being able to grasp spatial changing in the gas consumption distribution. Indeed, the fact that these "geographical" variation in consumption are completely uncorrelated one to another is extending the surrogate model capabilities to uncommon (hence out-of-domain) operating conditions. Usually, in fact, the gas consumption of final users belonging to the same network follows a common pattern (mainly related to outdoor climatic conditions) with a certain degree of individual variation. In any case, as the surrogate model has been trained on a much wider domain of variations with satisfactory results, the case described before can be seen as a subset of the overall scenarios which the model can address.

This wide generalization comes with a small loss of accuracy in the exact prediction of the hydrogen concentration in some specific nodes – the mixing ones and the nodes at the boundaries of the areas with homogeneous composition. In any case, the probability to make a very high prediction error on one of the critical nodes is very small as highlighted and commented in the RMSE discussion in paragraph 5.1.3. On the other hand, the accuracy on the predictions on the concentrations of nodes with homogeneous composition (equal to one of the sources) is very high. This means that the use of the surrogate model for defining areas of homogenous gas quality under a wide range of operating condition is reliable, as well as the identification of transitional areas and mixing areas, which deserves more attention.

From the global sensitivity analysis carried out on the nodes which displays the most complex behaviour, it is possible to draw that the nodal concentration is almost always primarily influenced by the concentration of one of the two sources. Among the fluid-dynamic parameters (pressure set-points and exiting gas flow rates) the pressure set-points are the one which influences the most with two nodes in which the sensitivity to the pressures is even higher than the concentration at the inlet points. These are nodes located in the middle of the area where moving boundaries are located. It is interesting to note that instead the nodal concentration in the investigated nodes is less affected by gas exit flows, with the highest sensitivity is towards the exit points in the surrounding of the investigated node. As an overall conclusion, one can draw that a part from the hydrogen concentration at the inlet nodes, the relative value of the pressure set points at the gas inlets influences the most the overall fluid dynamic equilibrium of the network hence the gas fluxes throughout the pipes which, in turn, are responsible for the further gas mixing within the infrastructure.

Comparing the network behaviour across the three case studies presented here shows that the 30 parameters case display a much more complex average distribution of hydrogen concentration, testifying an increased variability in the network response. However, the "critical" nodes and areas which were identified with the simpler cases are also critical in the 30 parameters case. In this latter case, it is as if the criticality zones are more diffused and can be displaced in the closer surroundings.

The research leading to these results has received funding from Horizon 2020, the European Union's Framework Programme for Research and Innovation (H2020) under grant agreement n° 101111888.

6 Conclusions

This deliverable demonstrates that the integration of vector-valued surrogate modelling with statistical and sensitivity analysis provides a robust and scalable framework for understanding hydrogen blending behaviour in gas networks. Beyond the validation of a machine-learning approach for accelerating parametric studies, the key added value lies in the systematic generalization of gas quality tracking results across wide operational domains, including out-of-domain scenarios that would be computationally prohibitive with physics-based simulations alone.

A first major conclusion is methodological. The proposed compressed vector-valued Kernel Ridge Regression (KRR) framework proves capable of reproducing the high-dimensional fluid-dynamic network responses—most notably nodal pressures, pipe flow rates/velocities, and the nodal mass exchanges required by the quality-tracking formulation—with high accuracy using a limited number of training samples. Based on these surrogate predictions, hydrogen concentrations are then computed through the dedicated mixing module, enabling fast network-wide quality mapping without running additional high-fidelity simulations. Even when increasing the number of uncertain parameters from 4 to 30, the overall surrogate-based workflow retains predictive capability while reducing computational time by orders of magnitude. This shift transforms parametric exploration from a case-by-case engineering exercise into a statistically grounded and computationally efficient process. As a consequence, network operators can complement deterministic scenario testing with probabilistic and sensitivity-based assessments of hydrogen injection strategies over broad operating domains.

A second conclusion concerns the structural behaviour of hydrogen distribution within looped networks. Across all investigated cases, the network consistently exhibits the emergence of quasi-homogeneous gas quality areas, separated by transitional zones where mixing conditions depend on the fluid-dynamic equilibrium. These areas are governed by the interplay between inlet pressure setpoints hierarchy, consumption patterns, and hydrogen concentration at injection points. Even when the dimensionality of the parameter space increases substantially, the critical zones identified in simpler cases persist, although their spatial extension and statistical relevance may vary. This confirms that hydrogen propagation is strongly topology-driven and that mixing boundaries tend to localize along specific structural interfaces of the network, particularly near loop interconnections.

A third important result concerns the quantification of uncertainty. By leveraging the surrogate model for large-scale Monte Carlo simulations, it becomes possible to map not only average hydrogen concentration patterns but also their variability and probability distributions. The identification of nodes with stable composition, permanently mixed behaviour, or state-switching characteristics (i.e., nodes belonging to moving boundaries) provides actionable insight for gas quality management. In particular, transitional nodes—where concentration may alternately reflect one source or a mixing regime—represent the most sensitive points from a monitoring and regulatory perspective. The statistical characterization of these nodes allows operators to estimate the likelihood of concentration shifts and to design monitoring systems accordingly.

Global Sensitivity Analysis further clarifies the hierarchy of influencing factors. The hydrogen concentration at injection points remains the dominant driver of nodal composition in most scenarios. However, inlet pressure set-points emerge as the most influential fluid-dynamic control variable, often exceeding the impact of localized consumption variations. This highlights a key operational insight: while hydrogen blending percentage defines the source composition, the pressure balance between entry points largely determines the spatial propagation and mixing structure within the network. Consumption clusters contribute mainly at a local level, particularly near the investigated nodes, but rarely dominate the global concentration behaviour. Pipe roughness, within the explored ranges, plays a negligible role in concentration variability.

The out-of-domain analysis confirms that increasing the dimensionality of independent variations leads to more diffuse and complex mixing regions. Nevertheless, even under fully uncorrelated pressure and

The research leading to these results has received funding from Horizon 2020, the European Union's Framework Programme for Research and Innovation (H2020) under grant agreement n° 101111888.

consumption variations, the surrogate-based approach maintains sufficient accuracy to identify homogeneous areas and critical transitional zones. The slight degradation in pointwise prediction accuracy observed in highly complex scenarios does not compromise the reliability of the statistical indicators that are most relevant for operational decision-making.

From a system-level perspective, the framework developed in this deliverable enables a shift toward smart network operation. By combining fast surrogate prediction, probabilistic evaluation, and sensitivity metrics, Gas Network Operators can:

- anticipate how hydrogen blending variability propagates spatially;
- identify stable gas quality regions suitable for simplified monitoring strategies;
- detect moving boundaries requiring enhanced supervision;
- evaluate the robustness of operational set-points before implementation.

In this sense, the contribution goes beyond computational acceleration: it provides a decision-support methodology for hydrogen injection management under uncertainty.

6.1 Further Work

Future developments should extend the present steady-state framework toward dynamic analyses, incorporating temporal evolution of demand, injection profiles, quality tracking through time. Additionally, integrating realistic correlations among consumption clusters would allow narrowing the explored domain toward a more realistic yet statistically representative operational scenarios while retaining the capability for stress-testing extreme conditions.

A particularly promising direction concerns the integration of the surrogate-based framework into optimization and control problems. Owing to its negligible computational cost once trained, the surrogate model can be embedded within optimization algorithms aimed at identifying optimal operating set-points for hydrogen injection and inlet pressures. For instance, the methodology could be used to determine the admissible variation ranges of pressure set points or hydrogen blending fractions that prevent the displacement of composition boundaries beyond predefined network zones. In this perspective, the moving boundaries identified in this deliverable become controllable features rather than passive consequences of operation.

More generally, the surrogate model enables the formulation of inverse problems in which the desired gas quality distribution (e.g., minimization of concentration variability in specific areas, containment of mixing within predefined regions, or stabilization of transitional nodes) is translated into constraints on operational parameters. This opens the way to model-based decision-support tools for proactive gas quality management, supporting Distribution and Transmission System Operators in maintaining stable and predictable hydrogen concentration profiles across the network.

Finally, testing the methodology on additional real DSO/TSO networks with different topologies will help assess the transferability of the identified mixing patterns and validate the generalization capability demonstrated in this deliverable.

The research leading to these results has received funding from Horizon 2020, the European Union's Framework Programme for Research and Innovation (H2020) under grant agreement n° 101111888.

7 References

[1] V. Sharma, Ü. Cali, B. Sardana, M. Kuzlu, D. Banga, and M. Pipattanasomporn, "Data-driven short-term natural gas demand forecasting with machine learning techniques", *Journal of Petroleum Science and Engineering,* 206, 108979 (2021).

[2] Z. Zhao, M. Guo, L. Fan, L. Han, Q. Yu, and Z. Wang, "Short-term natural gas load forecasting based on EL-VMD-Transformer-ResLSTM", *Scientific Report* ,14, 20343 (2024).

[3] J. Zhao J, Y. Bai, J. Li, W. Cu, W. Zhou, and Y. Zhang, "A leakage detection method for hydrogen-blended natural gas pipelines in utility tunnels based on multi-task LSTM and CFD simulation", *International Journal Hydrogen Energy,* 97:1335–47 (2025).

[4] J. Cristello, Z. Dang, R. Hugo, SS. Park, "Artificial intelligence-based leak detection in blended hydrogen and natural gas pipelines", *International Journal Hydrogen Energy,* 91:744–64 (2024).

[5] E. Ogbe, U. Mukherjee, M. Fowler, A. Almansoori, and A. Elkamel, "Integrated Design and Operation Optimization of Hydrogen Commingled with Natural Gas in Pipeline Networks", *Ind Eng Chem Res*, 59:1584–95 (2020).

[6] N. Soleimani, R. Trinchero, and F. G. Canavero, "Bridging the gap between artificial neural networks and kernel regressions for vector-valued problems in microwave applications," *IEEE Transactions on Microwave Theory and Techniques*, vol. 71, no. 6, pp. 2319–2332 (2023).

[7] E. Vaccariello, R. Trinchero, I.S. Stievano, P. Leone, "A statistical assessment of blending hydrogen into gas networks", *Energies*, 14(16), 5055 (2021).

[8] E. Vaccariello, R. Trinchero, P. Leone, and I.S. Stievano, "Synthetic gas networks for the statistical assessment of low-carbon distribution systems", *Sustainable Energy, Grids and Networks*, 31, 100765, (2022).

The research leading to these results has received funding from Horizon 2020, the European Union's Framework Programme for Research and Innovation (H2020) under grant agreement n° 101111888.

The research leading to these results has received funding from Horizon 2020, the European Union's Framework Programme for Research and Innovation (H2020) under grant agreement n° 101111888.

A Appendix A

A.1 Compressed Vector-Valued Kernel Ridge Regression (KRR)

The problem of modelling the parametric behavior of multiple output responses as a function of a (common) set of input parameters can be formulated as the learning of D scalar functions $\hat{f}^{(d)}: \mathcal{X} \to \mathcal{Y}$, for $d = 1, \dots, D$, using a training dataset [6]:

$$\mathcal{S} = \{(\boldsymbol{x}_\ell, \boldsymbol{y}_\ell)\}_{\ell=1}^{L},$$

where each input vector $\boldsymbol{x}_\ell \in \mathcal{X} \subset \mathbb{R}^p$ represents design or geometrical parameters and each output vector $\boldsymbol{y}_\ell \in \mathcal{Y} \subset \mathbb{R}^D$ collects the system responses under modeling (e.g., the pressure at each node of the network). I it important to notice that in the class of problems at hand (i.e. gas networks) D is large, typically on the order of hundreds.

In this modeling framework, the objective is to construct a vector-valued regression model capable of jointly predicting all D responses for new input configurations. The learning problem can be formulated as the minimization of a regularized least-squares cost functional [6] (and the references therein):

$$\hat{\mathbf{f}} = \arg\min_{\tilde{\mathbf{f}} \in \mathcal{H}} \sum_{d=1}^{D} \sum_{\ell=1}^{L} \left(y_\ell^{(d)} - \tilde{f}^{(d)}(\boldsymbol{x}_\ell) \right) + \lambda \left\| \tilde{\mathbf{f}} \right\|_{\mathcal{H}}^2,$$

where the first term measures the fitting error over all outputs and samples, while the second term, controlled by the regularization parameter λ, penalizes overly complex functions.

According to the representer theorem, the optimal solution can be expressed as a finite expansion in terms of the training samples:

$$\hat{\tilde{f}}(\boldsymbol{x}) = \sum_{\ell=1}^{L} \boldsymbol{K}(\boldsymbol{x}, \boldsymbol{x}_\ell) \boldsymbol{c}_\ell$$

where $\boldsymbol{K}(\boldsymbol{x}, \boldsymbol{x}_\ell)$ is a $D \times D$ positive semidefinite matrix-valued kernel encoding similarities in the input space and correlations among output components, while $\boldsymbol{c}_\ell \in \mathbb{R}^D$ are coefficient vectors.

A separable kernel structure is adopted, where the kernel is expressed as $\boldsymbol{K}(\boldsymbol{x}, \boldsymbol{x}') = k_x(\boldsymbol{x}, \boldsymbol{x}')\mathbf{B}$. Here, $k_x(\boldsymbol{x}, \boldsymbol{x}')$ measures input similarity and $\mathbf{B} \in \mathbb{R}^{D \times D}$ models correlations among outputs. Both must be positive semidefinite.

The matrix formulation of the problem leads to minimizing $\|\mathbf{Y} - \mathbf{K}_x \mathbf{C} \mathbf{B}\|_F^2 + \lambda \langle \mathbf{C}^T \mathbf{K}_x \mathbf{C}, \mathbf{B} \rangle_F$, yielding the Sylvester equation:

$$\mathbf{K}_x \mathbf{C} \mathbf{B} + \lambda \mathbf{C} = \mathbf{Y}$$

Solving the above Sylvester equation directly requires inverting an $LD \times LD$ matrix, which is computationally demanding. To reduce the cost, low-rank approximations are introduced:

$$\mathbf{K}_x \approx \mathbf{U}_r \boldsymbol{\Lambda}_r \mathbf{U}_r^T, \qquad \mathbf{B} \approx \mathbf{T}_n \mathbf{M}_n \mathbf{T}_n^T$$

Restricting the coefficient matrix to r- and n-dimensional subspaces yields

$$\mathbf{C} \approx \mathbf{U}_r \tilde{\mathbf{C}}_{r \times n} \mathbf{T}_n^T.$$

Substituting the above low-rank approximations of $\mathbf{K}_x$ and $\mathbf{B}$, together with the approximation of the coefficient matrix, the original Sylvester equation can be recast as the following reduced system:

The research leading to these results has received funding from Horizon 2020, the European Union's Framework Programme for Research and Innovation (H2020) under grant agreement n° 101111888.

$$\mathbf{\Lambda}_r \, \tilde{\mathbf{C}}_{r\times n} \, \mathbf{M}_n + \lambda \, \tilde{\mathbf{C}}_{r\times n} = \tilde{\mathbf{Y}},$$

where $\tilde{\mathbf{Y}} = \mathbf{U}_r^T \, \mathbf{Y} \, \mathbf{T}_n$.

Because $\mathbf{\Lambda}_r$ and $\mathbf{M}_n$ are diagonal, the system is decoupled into rn scalar equations of the form:

$$\lambda_i \, \tilde{C}_{ij} \, m_j + \lambda \, \tilde{C}_{ij} = \tilde{Y}_{ij}.$$

Each reduced coefficient can be computed as $\tilde{C}_{ij} = \tilde{Y}_{ij} \, / \, (\lambda_i \, m_j + \lambda)$, providing an explicit expression for each entry of the reduced coefficient matrix. All coefficients are computed independently, without matrix inversion, ensuring numerical stability and computational efficiency.

The prediction for a new input $\boldsymbol{x}^*$ is obtained as $\hat{\mathbf{f}}(\boldsymbol{x}^*)^T = k_x(\boldsymbol{x}^*, \mathbf{X}) \, \mathbf{U}_r \, \tilde{\mathbf{C}}_{r\times n} \, \mathbf{T}_n^T \, \mathbf{B}$. This formulation provides compact, efficient, and numerically stable evaluations without reconstructing full kernel matrices.

A.2 Machine Learning Workflow as Pseudocode

The procedure for generating a ML model for the above network is reported below, with a pseudo-code that allows implementing the following flow:

(A) **Initialization**

- Set and define the variables of the solver (if needed).
- Define the number of training samples: `N_ED`.
- Define the number of test samples: `N_TEST`.
- Define the number of input variables/parameters: `N_param`.
- Define the vector `Delta` of size (`N_param × 1`) collecting the relative variability `Delta_i` associated with each input variable/parameter.
- Generate `N_ED` normalized realizations of the input variables/parameters (i.e., $x_i \in [-1, 1]$ for $i = 1, \ldots,$ `N_param`) for the training set, drawn according to their corresponding statistical distributions, and store them in matrix `X_ED` of size (`N_ED x N_param`).
- Generate `N_TEST` normalized realizations of the input variables/parameters (i.e., $x\_i \in [-1, 1]$ for $i = 1, \ldots,$ `N_param`) for the test set, drawn according to their corresponding statistical distributions, and store them in matrix `X_TEST` of size (`N_TEST x N_param`)

(A) **Data Collection**

Training Set

Generate the output samples for the training set by running multiple simulations with the selected solver.

- Set `counter_train = 0`.
- For `jj = 1:N_ED`:
  - Compute the actual values of the input variables in vector `X`, such that: `X = X0 + Delta .* X_ED(jj,:)`, where the vector `X0` collects the mean values associated with each input variable/parameter
  - Call the solver: `[output, error] = OpenNetSsolver(X, U)`
  - If no error:

The research leading to these results has received funding from Horizon 2020, the European Union's Framework Programme for Research and Innovation (H2020) under grant agreement n° 101111888.

- Increment `counter_train` by 1.
- Optionally post-process the output.
- Save the output in matrix `Y_ED`, i.e., `Y_ED(counter_train,:) = output`.

- End loop.

Test Set

Generate the output samples for the test set by running multiple simulations with the selected solver.

- Set `counter_test = 0`.
- For `jj = 1:N_TEST`:
  - Compute the actual values of the input variables in vector `X`, such that: `X = X0 + Delta .* X_TEST(jj,:) )`, where the vector `X0` vector collects the mean values associated with each input variable/parameter
  - Call the solver: `[output, error] = OpenNetSolver(X, U)`
  - If no error:
    - Increment `counter_test` by 1.
    - Optionally post-process the output.
    - Save the output in matrix `Y_TEST`, i.e., `Y_TEST(counter_test,:) = output`.
- End loop.

(B) **Model Training**

- The obtained matrices `X_ED` and `Y_ED` are then used within the training scheme presented in the previous Section for the vector-valued ridge regression to build a surrogate model. For example: `[model] = train(X_ED, Y_ED)` (the algorithm [6] is implemented and used)
- In the considered implementation the model training includes estimating the model's coefficients and optimizing the hyperparameters using 5-fold cross-validation.

(C) **Surrogate Model Validation**

- Evaluate the ML model on the test set. For example: `[Y_pred] = predict(model, X_TEST)`
- Assess the model's performance using standard metrics and scatter plots. These metrics are computed using the test set `Y_TEST` and the corresponding model predictions in vector `Y_pred`.

(D) **Statistical Analysis** (see hereafter in this section for the considered Global Sensitivity Analysis)

- Use the validated model to perform a statistical analysis of the output variables.
- Analyze the behavior of the outputs based on the trained surrogate model.

The research leading to these results has received funding from Horizon 2020, the European Union's Framework Programme for Research and Innovation (H2020) under grant agreement n° 101111888.

The research leading to these results has received funding from Horizon 2020, the European Union's Framework Programme for Research and Innovation (H2020) under grant agreement n° 101111888.

The research leading to these results has received funding from Horizon 2020, the European Union's Framework Programme for Research and Innovation (H2020) under grant agreement n° 101111888.